Dissolved CH_4 coupled to Photosynthetic Picoeukaryotes in Oxic Waters and Cumulative Chlorophyll-a in Anoxia in Reservoirs

Elizabeth León-Palmero[1], Alba Contreras-Ruiz[1], Ana Sierra[2], Rafael Morales-Baquero[1], Isabel Reche[1,3]

[1]Instituto del Agua and Departamento de Ecología, Universidad de Granada, Granada, 18071, Spain

[2]Departamento de Química-Física and Instituto Universitario de Investigación Marina (INMAR), Facultad de Ciencias del Mar y Ambientales, Universidad de Cádiz, Puerto Real, 11510, Cádiz, Spain

[3]Research Unit Modeling Nature (MNat), Universidad de Granada, Granada, 18071, Spain

Correspondence to: Isabel Reche (ireche@ugr.es)

Abstract. Methane (CH_4) emissions from reservoirs are responsible for most of the atmospheric climatic forcing of these aquatic ecosystems, comparable to emissions from paddies or biomass burning. Primarily, CH_4 is produced during the anaerobic mineralization of organic carbon in anoxic sediments by methanogenic archaea. However, the origin of the recurrent and ubiquitous CH_4 supersaturation in oxic waters (i.e., the methane paradox) is still controversial. Here, we determined the dissolved CH_4 concentration in the water column of twelve reservoirs during summer stratification and winter mixing to explore CH_4 sources in oxic waters. Reservoirs size ranged from 1.18 to 26.13 km^2. We obtained that dissolved CH_4 in the water column varied up to four orders of magnitude (0.02-213.64 μM), and all oxic depths were consistently supersaturated in both periods. Phytoplanktonic sources appear to determine the concentration of CH_4 in these reservoirs primarily. In anoxic waters, the depth-cumulative chlorophyll-a concentration, a proxy for the phytoplanktonic biomass exported to sediments, was correlated to CH_4 concentration. In oxic waters, the photosynthetic picoeukaryotes abundance was significantly correlated to the dissolved CH_4 concentration both during the stratification and the mixing. The mean depth of the reservoirs, as a surrogate of the vertical CH_4 transport from sediment to the oxic waters, also contributed notably to the CH_4 concentration in oxic waters. Our findings suggest that photosynthetic picoeukaryotes can have a significant role in determining CH_4 concentration in oxic waters, although their role as CH_4 sources to explain methane paradox has been poorly explored.

1 Introduction

Lakes and reservoirs are significant sources of methane (CH_4), affecting the atmospheric climatic forcing (Deemer et al., 2016). The estimated contribution of lakes to global emission budget is ca. 71.6 Tg CH_4 $year^{-1}$ (Bastviken et al., 2011), and the specific contribution of reservoirs ranges between 4 and 70 Tg CH_4 $year^{-1}$, representing up to 10 % of total CH_4 emissions (Deemer et al., 2016). Although freshwaters only cover about 5-8 % of the Earth´s surface (Mitsch et al., 2012),

they emit more CH_4 than the ocean surface (Saunois et al., 2016). Traditionally, the net CH_4 production is determined by archaeal methanogenesis, which produces methane as an end product of organic matter degradation in anoxic conditions, and to methanotrophs, which consume it in oxic conditions (Schubert and Wehrli, 2018). In freshwater ecosystems, the anoxic sediments are a primary source of CH_4 (Segers, 1998), where methanogens are very sensitive to temperature and quantity and quality of the organic matter used as substrate (Marotta et al., 2014; Rasilo et al., 2015; Sepulveda-Jauregui et al., 2018; Thanh-Duc et al., 2010; West et al., 2012; Yvon-Durocher et al., 2014). They are also affected by the extent of anoxia in the sediments, as far as they are obligate anaerobes and will not survive and produce CH_4 under aerobic conditions (Chistoserdova et al., 1998; Schubert and Wehrli, 2018). However, many observations from freshwaters and marine waters have detected CH_4 supersaturation in the oxic layers. A widespread phenomenon described as the "methane paradox" (Bogard et al., 2014; Damm et al., 2010; Donis et al., 2017; Grossart et al., 2011; Kiene, 1991; Murase et al., 2003; Owens et al., 1991; Schmidt and Conrad, 1993; Schulz et al., 2001; Tang et al., 2014, 2016).

This persistent CH_4 supersaturation in oxic layers of marine and freshwater ecosystems requires extra inputs to compensate for the CH_4 losses by methanotrophy and the emissions toward the atmosphere. CH_4 inputs may come from anoxic sediments or from *in situ* sources in the oxic layers. The transport of CH_4 from the bottom and littoral sediments in shallow zones has been proposed to explain the supersaturation in the surface waters of some lakes (Bastviken et al., 2004; Encinas Fernández et al., 2016; Michmerhuizen et al., 1996; Murase et al., 2003; Peeters et al., 2019; Rudd and Hamilton, 1978). The vertical transport may be relevant in small lakes, but in deep and thermally stratified systems, the vertical diffusion rates of dissolved gases across the thermocline are too low, and there is not apparent CH_4 upward movements from the hypolimnion (Peeters et al., 1996; Rudd and Hamilton, 1978). In fact, Thalasso et al. (2020) determined that there was no exchange between the hypolimnion and the epilimnion in a Siberian lake. The CH_4 produced in the sediments and the hypolimnion was assimilated there. Consequently, the CH_4 in the epilimnion came from lateral transport and *in situ* production. Lateral CH_4 transport from shallow sediments of the littoral zones may be a significant source in the open surface of some lakes and reservoirs. DelSontro et al. (2018) resolved that CH_4 transport from littoral zones was relevant for the dissolved CH_4 in the epilimnion of small lakes. However, lateral transport does not fully explain CH_4 supersaturation in the open ocean, and large freshwater ecosystems, hence, other *in situ* CH_4 sources likely occur (Damm et al., 2010; DelSontro et al., 2018; Grossart et al., 2011; Khatun et al., 2020; Owens et al., 1991; Schmidt and Conrad, 1993; Schulz et al., 2001; Scranton and Brewer, 1977; Tang et al., 2014; Tilbrook and Karl, 1995).

Previous works demonstrated the in situ CH_4 production in oxic waters using stable isotope techniques in experiments, mesocosms, and field samples (Bižić et al., 2020; Bogard et al., 2014; DelSontro et al., 2018; Hartmann et al., 2020; Tang et al., 2016) and using molecular approaches (Grossart et al., 2011; Khatun et al., 2020; Yao et al., 2016a). In the literature, there are different alternatives proposed as CH_4 sources. On the one hand, the occurrence of methanogenesis in micro-anoxic niches in the guts of zooplankton, and within sinking particles (Angelis and Lee, 1994; Karl and Tilbrook, 1994). In both micro-niches, the CH_4 production appeared to be too low to sustain the total CH_4 supersaturation of the oxic waters (Schmale et al., 2018; Tang et al., 2014). On the other hand, there is a consistent link between dissolved CH_4

concentration and autotrophic organisms, primary production, and chlorophyll-a concentration (Bogard et al., 2014; Grossart et al., 2011; Owens et al., 1991; Schmidt and Conrad, 1993; Tang et al., 2014). Grossart et al., (2011) detected potential methanogenic *Archaea* attached to photoautotrophs as *Chlorophyta* (*Eukarya*) and *Cyanobacteria* (*Bacteria*) in the epilimnion of an oligotrophic lake and confirmed the production of CH_4 in the presence of oxygen in laboratory incubations. If occurring, that symbiosis would require that the methanogenic microorganisms tolerate the oxygen exposure as it has been observed by several authors (Angel et al. 2011; Angle et al., 2017; Jarrell, 1985), in contrast to general belief. New findings suggest that the link between phytoplankton and dissolved CH_4 may rely on diverse metabolic pathways in *Bacteria* and *Eukarya*. These metabolic pathways contribute to the dissolved CH_4 in oxic waters due to the degradation of methylated compounds. In the open ocean, archaea and bacteria appear to metabolize the algal osmolyte dimethylsulfoniopropionate producing methane as a by-product (Damm et al., 2008, 2010, 2015; Zindler et al., 2013). Common methyl-containing substances as methionine produce methane in algae, saprotrophic fungi, and plants (Lenhart et al., 2012, 2015, 2016). Another reported pathway is the degradation of methyl-phosphonates (MPn) as an alternative source of phosphorus (P) in phosphate-starved bacterioplankton. The hydrolysis of these compounds, using the enzyme C–P lyase, also releases methane as a by-product. This pathway appears in chronically P starved ecosystems as the ocean gyres, oligotrophic lakes, and microbial mats (Beversdorf et al., 2010; Carini et al., 2014; Gomez-Garcia et al., 2011; Karl et al., 2008; Repeta et al., 2016; Teikari et al., 2018; del Valle and Karl, 2014; Wang et al., 2017; Yao et al., 2016a). Recent studies using phytoplankton cultures and stable isotope techniques propose that the production of CH_4 may rely directly on the photoautotrophic carbon fixation of algae and *Cyanobacteria* (Bižić et al., 2020; Hartmann et al., 2020; Klintzsch et al., 2019; Lenhart et al., 2016). These sources of CH_4 in oxic waters, however, still have not been tested simultaneously in reservoirs, despite the known high contribution of these freshwater ecosystems to global CH_4 emissions.

In this study, we measured the dissolved CH_4 concentration in the water column of twelve reservoirs that cover a broad spectrum of sizes, ages, morphometries, and trophic states during the summer stratification and winter mixing (León-Palmero et al., 2020). Our objective was to assess the relative contribution of different sources of CH_4 in the oxic waters and to shed light on the methane paradox depending on reservoir properties. We explored the following CH_4 sources in oxic waters: 1) vertical and lateral transport of CH_4 from hypolimnetic and littoral waters; 2) *in situ* production by methanogenic *Archaea* tolerant to oxygen; 3) *in situ* production by methylphosphonate degradation; 4) *in situ* production by photosynthetic microorganisms. We used the concentration chlorophyll-a, the primary productivity and the abundance of photosynthetic picoeukaryotes and cyanobacteria as variables for the photosynthetic signatures. The photosynthetic picoeukaryotes are a relevant part of the freshwater phytoplankton, but their role in the methane paradox has been particularly little studied.

2 Methods

2.1 Study Reservoirs, Morphometry, and Vertical Profiles

We sampled twelve reservoirs located in the southern Spain (Figure 1) between July 2016 and August 2017 once during the summer stratification and once during winter mixing. In Table 1, we show the geographical coordinates, age, and the morphometry description of the study reservoirs. The reservoirs were built between 1932 and 2003, for water supply and agriculture irrigation, and they are located in watersheds with different lithology and land-use (more details can be found in León-Palmero et al. 2019, 2020). These reservoirs differ in morphometric, chemical, and trophic characteristics covering a wide range of concentrations of dissolved organic carbon (DOC), total nitrogen (TN), total phosphorus (TP), and chlorophyll-a (Table 2). All raw data for the water column was deposited in Pangaea database (https://doi.org/10.1594/PANGAEA.912535).

We obtained the reservoir surface area, perimeter, and volume using the following open databases: Infraestructura de Datos Espaciales de Andalucía (IDEAndalucia; http://www.ideandalucia.es/portal/web/ideandalucia/), and the Ministerio para la Transición Ecológica (https://www.embalses.net/).

The mean depth was calculated as follows (Eq. 1):

$$\text{Mean depth (m)} = \frac{\text{Volume (m}^3\text{)}}{\text{Surface area (m}^2\text{)}}, \quad (1)$$

The shoreline development ratio (D_L) (Aronow, 1982) is a comparative index relating the shoreline length (i.e., the perimeter of the reservoir) to the circumference of a circle that has the same area. The closer this ratio is to 1, the more circular the lake. A large ratio (>>1) indicates the shoreline is more scalloped than a low ratio. The equation is as follows (Eq. 2):

$$D_L = \frac{\text{Length of the shoreline (m)}}{2\sqrt{\pi\ \text{Area (m}^2\text{)}}}, \quad (2)$$

The shallowness index (m^{-1}) was obtained by dividing the shoreline development index (D_L) by the mean depth (m), as follows in eq. 3:

$$\text{Shallowness index (m}^{-1}\text{)} = \frac{D_L}{\text{Mean depth (m)}} \quad (3)$$

We sampled the water column near the dam, in the open waters of the reservoir. During the stratification and the mixing period, we selected the same location. First, we performed a vertical profile of the reservoir using a Seabird 19plus CTD profiler, coupled to Spherical Underwater Quantum Sensor (LI-193R), and a fluorimeter Turner® SCUFA (model CYCLOPS–7) for continuous measurements of temperature (ºC), dissolved oxygen (µM), conductivity (µS/cm), turbidity (FTU), density (kg m^{-3}), photosynthetic active radiation, chlorophyll-a fluorescence (µg L^{-1}), specific conductance (µS/cm), and salinity (psu). Then, based on the temperature and oxygen profiles, we selected from 6 to 9 depths representative of the oxic, anoxic layers, and the transition between them in the different reservoirs. We took the water samples using a UWITEC sampling bottle of 5 liters with a self-closing mechanism. We collected samples for the dissolved CH_4 analysis in 125 or 250 mL air-tight Winkler bottles by duplicate (250 mL) or triplicate (125 mL). We filled up the bottles very carefully from the bottom to avoid the formation of bubbles and minimize the loss of CH_4 during field sampling. We preserved the samples

with a solution of $HgCl_2$ (final concentration 1mM) to inhibit biological activity and sealed the bottles with Apiezon® grease to prevent gas exchanges. We also took samples from each depth to the chemical and biological analysis explained below. We also measured barometric pressure using a multi-parameter probe (HANNA HI 9828) for the gas saturation calculations. We calculated the saturation values (%) for dissolved oxygen as the ratio of the dissolved gas measured and the gas concentration expected in equilibrium. We calculated the gas concentration in equilibrium, taking into account the differences in temperature, salinity, and barometric pressure (Mortimer, 1956).

2.2 Dissolved CH_4 in the water column

We stored the Winkler bottles in the dark at room temperature until analysis in the laboratory. We measured dissolved CH_4 using headspace equilibration in a 50 ml air-tight glass syringe (Agilent P/N 5190–1547) (Sierra et al., 2017). We obtained two replicates for each 150 mL Winkler bottle, and three replicates for each 250 mL Winkler bottle. We took a quantity of 25 g of water (± 0.01 g) using the air-tight syringe and added a quantity of 25 mL of a standard gas mixture that had a methane concentration similar to atmospheric values (1.8 ppmv) to complete the volume of the syringe. The syringes were shaken for 5 min (VIBROMATIC Selecta) to ensure mixing, and we waited 5 min to reach complete equilibrium. Then, the gas in the syringe was injected manually in the gas chromatograph (GC; Bruker® GC-450) equipped with Hydrogen Flame Ionization Detector (FID). We daily calibrated the detectors using three standard gas mixtures with CH_4 mixing ratios of 1952, 10064, 103829 ppbv, made and certified by Air Liquide (France). The precision in the quantification of the gas mixture of CH_4 used in the headspace equilibrium (1.8 ppmv) expressed as the coefficient of variation was 3.7% (n = 123). The precision of the measurement of the dissolved CH_4 concentration, that included the analytical processing of the samples and the equilibration step, was 3.6% for four to six replicates of each sample. We calculated the saturation values (%) as the ratio between the concentration of the dissolved gas measured and the gas concentration expected in equilibrium considering the temperature, salinity, and barometric pressure of each reservoir. We calculated the gas concentration in equilibrium using the Bunsen functions for CH_4 (Wiesenburg and Guinasso, 1979; Yamamoto et al., 1976). We used the atmospheric gas concentrations provided by *The Global Greenhouse Gas Reference Network* website (https://www.esrl.noaa.gov/gmd/ccgg/index.html), which is part of the National Oceanic and Atmospheric Administration (NOAA) Earth System Research Laboratory in Boulder, Colorado. We calculated the 2016 global mean atmospheric concentrations for CH_4 (Dlugokencky, 2019) from the 2016 global monthly mean. The differences among these values and the local atmospheric concentrations are assumed to be small compared with the high dissolved concentrations obtained in the study reservoirs.

2.3 Chemical analysis in the water column

From the discrete sampling, we selected 3 or 4 representative depths of the epilimnion, metalimnion (oxycline), and hypolimnion/bottom layers for nutrient analysis during the stratification period. We also selected 3 or 4 equivalent depths during the mixing period. In total, we analyzed 77 samples: 41 samples from the stratification period, and 36 samples from

the mixing period. We determined total nutrients using unfiltered water, while we filtered the samples through pre-combusted 0.7-µm pore-size Whatman GF/F glass-fiber filters for the dissolved nutrients. We acidified the samples for dissolved organic carbon (DOC), total dissolved nitrogen (TDN), and total nitrogen (TN) samples with phosphoric acid (final pH<2). We measured DOC, TN, and TDN by high–temperature catalytic oxidation using a Shimadzu total organic carbon (TOC) analyzer (Model TOC-V CSH) coupled to a nitrogen analyzer (TNM-1). We calibrated the instrument using a four-point standard curve of dried potassium hydrogen phthalate for DOC, and dried potassium nitrate for TN and TDN (Álvarez-Salgado and Miller, 1998). We analyzed two replicates and three to five injections per replicate for each sample. We purged the DOC samples with phosphoric acid for 20 min to eliminate all the dissolved inorganic carbon. The precision of the DOC measurements expressed as the mean coefficient of variation was 3.0%. The mean precision for the TN and TDN was 8.2% and 2.9%, respectively.

We measured the NO_3^- concentration by duplicate using the ultraviolet spectrophotometric method, using a Perkin Elmer UV-Lambda 40 spectrophotometer at wavelengths of 220 nm and correcting for DOC absorbance at 275 nm (Baird et al., 2012). The mean coefficient of variation was 0.5%. We measured $NH_4^+$and NO_2^- concentrations by Inductively Coupled Plasma Optical Emission Spectrometry (ICP-OES). Dissolved inorganic nitrogen (DIN) was calculated as the addition of the NO_3^-, NH_4^+, and NO_2^- concentrations. The detection limit for the NH_4^+, and NO_2^- concentrations were 3.6 µM and 1.4 µM, respectively. We measured total phosphorus (TP) concentration by triplicate using the molybdenum blue method (Murphy and Riley, 1962) after digestion with a mixture of potassium persulphate and boric acid at 120 °C for 30 min (Baird et al., 2012). The precision in the quantification of the TP concentration was 11.1%.

2.4 Chlorophyll-a, Phytoplankton, and Primary Production in the water column

We determined the chlorophyll-*a* concentration, and the abundances of cyanobacteria and photosynthetic picoeukaryotes in all the depths sampled during the discrete samplings (n = 178). We determined the chlorophyll-*a* concentration by filtering the particulate material of 500 to 2000 ml of water through pre-combusted Whatman GF/F glass-fiber filters. Then, we extracted the pigments from the filters with 95% methanol in the dark at 4 °C for 24 h (Baird et al., 2012). We measured chlorophyll-a (Chl-a) absorption using a Perkin Elmer UV-Lambda 40 spectrophotometer at the wavelength of 665 nm and for scattering correction at 750 nm. The detection limit was 0.1 µg L^{-1}.

To obtain the cumulative chlorophyll-a in the whole water column (mg Chl-*a* m^{-2}), from the discrete depths, we summed the concentration of Chl-*a* from each stratum using the trapezoidal rule (León-Palmero et al., 2019), as indicated in the following equation (4):

$$\text{Cumulative Chla-a} = \sum_{k=1}^{n} X_{ik} * \left(Z_{k+1} - \frac{Z_{k-1}}{2}\right) \quad (4)$$

Where Z stands for the depth considered, and n is the number of depths sampled. Z_k stands for the *n* sampled depth; X_{ij} is the Chla-a concentration (µg L^{-1}) at the depth Z_k.

We determined by triplicate the abundances of cyanobacteria and photosynthetic picoeukaryotes using flow cytometry using unfiltered water. We collected and fixed the samples with a mixture of 1% paraformaldehyde and 0.05% glutaraldehyde for 30 min in the dark at 4 °C. Then, we froze the samples in liquid nitrogen and stored them at −80 °C until analysis. We analyzed the samples in the FACScalibur flow cytometer equipped with the BD CellQuest Pro software for data analysis. We used yellow-green 0.92 µm latex beads (Polysciences) as an internal standard to control the cytometer performance every day. We used different signals for groups determination: the side scatter (SSC), chlorophyll-a (red fluorescence, FL3), phycoerythrin (the orange fluorescence, FL2), and phycocyanin (the blue fluorescence, FL4); following the protocols and indications for data analysis of previous works (Cellamare et al., 2010; Collier, 2000; Corzo et al., 1999; Gasol and Giorgio, 2000; Liu et al., 2014). In figure S13, we show a cytogram of the populations of cyanobacteria and photosynthetic picoeukaryotes. The mean coefficient of variation for the abundances of cyanobacteria and photosynthetic picoeukaryotes was 8.8% and 11.4%, respectively.

We estimated gross primary production (GPP), net ecosystem production (NEP), and ecosystem respiration (R) by measuring temporal changes in dissolved oxygen concentration and temperature using a miniDOT (PME) submersible water logger during the stratification period. We recorded measurements every 10 minutes for 24-48 hours during the same sampling days. Briefly, the equation for estimating free-water metabolism from measurements of dissolved oxygen was established by Odum (1956) (equation 5):

$$\Delta O_2 / \Delta t = GPP - R - F - A \quad (5)$$

Where $\Delta O_2 / \Delta t$ is the change in dissolved oxygen concentration through time; F is the exchange of O_2 with the atmosphere; and A is a term that combines all other processes that may cause changes in the dissolved oxygen concentration as horizontal or vertical advection, and it is often assumed to be negligible. The calculations were performed as in Staehr et al., (2010). The physical gas flux was modelled as follows (equation 6):

$$F \left(g\ O_2\ m^{-2}\ h^{-1}\right) = k\ (O_{2\ meas} - O_{2\ sat}) \quad (6)$$

Where F is the physical gas flux, k (m h^{-1}) is the piston velocity estimated following the equation of Jähne et al., (1987) and the indications of Staehr et al., (2010). $O_{2\ meas}$ is the actual oxygen concentration (mg mL^{-1}), and $O_{2\ sat}$ is the oxygen concentration in water in equilibrium with the atmosphere at ambient temperature and salinity.

We calculated the hourly net ecosystem production (NEP_{hr}) and the daytime net ecosystem production ($NEP_{daytime}$) following the equations 7 (Cole et al., 2000) and 8:

$$NEP_{hr} \left(g\ O_2\ m^{-3}\ h^{-1}\right) = \Delta O_2 \left(g\ m^{-3}\ h^{-1}\right) - F/Z_{mix} \quad (7)$$

$$NEP_{daytime} \left(g\ O_2\ m^{-3}\ daylight\ period^{-1}\right) = \text{mean } NEP_{hr} \text{ during daylight } \left(g\ O_2\ m^{-3}\ h^{-1}\right) \text{ x Light hours (h)} \quad (8)$$

NEP_{hr} is directly derived from the changes in dissolved oxygen (ΔO_2), after accounting for physical gas flux with the atmosphere (F). Z_{mix} is the depth of the mixed layer (m), and that was inferred from the temperature profile as the upper mixed zone where the temperature remains constant. $NEP_{daytime}$ is the portion of NEP between sunrise and sunset, when the

photosynthesis is taking place. We obtained the exact light hours from an online solar calculator (https://es.calcuworld.com/calendarios/calcular-salida-y-puesta-del-sol/). We established the start and the end time for photosynthesis as 30 minutes before sunrise and 30 minutes after dawn (Schlesinger and Bernhardt, 2013). We obtained hourly R (R_{hr}), R during the daytime ($R_{daytime}$), and R during all the day (R_{day}) following equation 9, 10, and 11, respectively:

$$R_{hr}\left(g\ O_2\ m^{-3}\ h^{-1}\right) = \text{mean } NEP_{hr} \text{ during darkness } \left(g\ O_2\ m^{-3}\ h^{-1}\right) \quad (9)$$

$$R_{daytime}\left(g\ O_2\ m^{-3}\ \text{daylight period}^{-1}\right) = R_{hr}\left(g\ O_2\ m^{-3}\ h^{-1}\right) \text{ x Light hours (h)} \quad (10)$$

$$R_{day}\left(g\ O_2\ m^{-3}\ d^{-1}\right) = R_{hr}\left(g\ O_2\ m^{-3}\ h^{-1}\right) \text{ x 24 (h)} \quad (11)$$

We calculated the respiration rate during the night (the period between 60 minutes after dawn and 60 minutes before sunrise) (Staehr et al., 2010), and we assumed that the respiration rate overnight was similar to the respiration rate over the day. Finally, we obtained the GPP and NEP for the day (equation 12 and 13):

$$GPP\left(g\ O_2\ m^{-3}\ d^{-1}\right) = NEP_{daytime} + R_{daytime} \quad (12)$$

$$NEP\left(g\ O_2\ m^{-3}\ d^{-1}\right) = GPP - R_{day} \quad (13)$$

2.5 DNA analysis

We selected 3 or 4 representative depths for determining the abundance of the functional genes of the epilimnion, metalimnion (oxycline), and hypolimnion/bottom layers during the stratification period. We also selected 3 or 4 equivalent depths during the mixing period. In total, we analyzed 41 samples from the stratification period and 36 samples for the mixing period. We pre-filtered the water through 3.0 µm pore-size filters and extracted DNA following the procedure developed by Boström et al., (2004) for environmental samples. During the DNA extraction protocol, we combined a cell recovery step by centrifugation of 12 - 20 mL of the pre-filtered water, a cell lysis step with enzyme treatment (lysozyme and proteinase K), and finally, the DNA recovery step with a co-precipitant (yeast tRNA) to improve the precipitation of low-concentration DNA. DNA was quantified using a DNA quantitation kit (Sigma-Aldrich) based on the fluorescent dye bisBenzimide (Hoechst 33258). Extracted DNA served as the template for PCR and quantitative PCR (qPCR) analysis to test the presence and abundance of the *mcrA* gene and the *phnJ* gene. For PCR analysis, we used the recombinant Taq DNA Polymerase (Thermo Fisher Scientific) using the Mastercycler X50 thermal cycler (Eppendorf). We ran the qPCR plates using SYBR Green as the reporter dye (PowerUp™ SYBR™ Green Master Mix, Thermo Fisher Scientific) in the Applied Biosystems 7500 Real-Time PCR System and the 7500 Software. In both cases, PCR and qPCR, we designed the standard reaction mix recipes and the thermocycling conditions using the provider specifications and primer requirements. We chose specific primers from studies performed in natural samples of freshwaters. We used pure cultures as positive controls (more details below).

We targeted the alpha subunit of methyl-coenzyme reductase (*mcrA*) as a genetic marker to determine the existence and abundance of methanogenic *Archaea* in our samples. This gene appears to be an excellent marker since all known methanogens have the *methyl coenzyme-M reductase*, which is the enzyme responsible for the conversion of a methyl group to CH_4 (Grabarse et al., 2001). We used specific primers from West et al. (2012) adapting their procedure. The forward primer was mcrAqF (5'-AYGGTATGGARCAGTACGA-3'), and the reverse primer was mcrAqF (5'-TGVAGRTCGTABCCGWAGAA -3'), and the annealing temperature was 54 ºC. The expected size of the PCR product was ~200 bp. We used a culture of *Methanosarcina acetivorans* (ATCC 35395) as a positive control. We tested all the samples (n=77). We also tested the presence of the *phnJ* gene, which encodes a subunit of the C-P lyase complex (Seweryn et al., 2015; White and Metcalf, 2007). This enzyme cleaves C-P bonds in phosphonate compounds releasing methane, and changes in response to the phosphate availability (Yao et al., 2016a). We ran the amplification with a pair of primers previously used by Fox et al., (2014); and Yao et al., (2016a). The forward primer was PhnJoc1 (5'-AARGTRATMGAYCARGG-3') and the reverse PhnJoc2 (5'-CATYTTYGGATTRTCRAA-3') adapting the PCR procedure from Yao et al., (2016a). The annealing temperature was 52.5 ºC, and the positive controls were run using a pure culture of *Rhodopseudomonas palustris* (ATCC 33872). The expected size of the PCR product was ~400 bp. We checked the result of the amplification by running 1.5 % (w/v) agarose gel electrophoresis. If we did not detect amplification in the PCR or qPCR samples, we changed the standard procedure by increasing the DNA amount and the primers concentration to corroborate the negative results. We tested all the samples (n=77).

2. 6. Statistical tests

We conducted all the statistical analysis in R (R Core Team, 2014) using the packages car (Fox and Weisberg, 2011), nortest (Gross and Ligges, 2015), and mgcv (Wood, 2011). We performed the Shapiro-Wilk test of normality analysis and Levene's test for homogeneity of variance across groups. We performed a one-way analysis of variance test (ANOVA) when the data were normally distributed. In case the data did not meet the assumptions of normality, we used the paired Kruskal-Wallis rank-sum (K-W) or Wilcoxon (V) tests. We analyzed the potential sources of dissolved CH_4 using simple regression analysis and generalized additive models (GAMs) (Wood, 2006). GAM is a generalized model with a linear predictor involving a sum of smooth functions of covariates (Hastie and Tibshirani, 1986, 1990). The model structure is shown in Eq. (4):

$$y_i = f_1(x_{1i}) + f_2(x_{2i}) + \cdots + f_n(x_{ni}) + \in_i , \quad (4)$$

Where the f_j are the smooth functions, and the $\in_i$ are independent identically distributed $N\ (0, \sigma^2)$ random variables. We fit smoothing functions by penalized cubic regression splines. The cross-validation method (Generalized Cross Validation criterion, GCV) estimates the smoothness of the functions. We fitted the models to minimize the Akaike Information Criterion (AIC) and the GCV values. We calculated the percentage of variance explained by the model (adj R^2) and the quality of the fit (deviance explained). We also fixed the effect of each predictor to assess the contribution of the other

predictor on the total deviance explained. Then, the sum of the deviance explained by two predictors can be different from the deviance explained by the model due to interactive effects.

3 Results and discussion

3. 1. Profiles description

We found pronounced differences in the concentration of dissolved CH_4 of the study reservoirs among depths and seasonal periods (Figs 2-4, Figs S1-9). The concentration of dissolved CH_4 ranged up to four orders of magnitude from 0.06 to 213.64 µM during the summer stratification (n = 96), and it was less variable during the winter mixing (n = 84) ranging only from 0.02 to 0.69 µM. All depths were consistently supersaturated in CH_4 both during the stratification and mixing period (Table S1). The dissolved CH_4 concentration and the % of saturation values were significantly higher during the stratification period than during the mixing period (V = 78, p-value < 0.001; V = 78, p-value < 0.001, respectively). These differences in the concentration of dissolved CH_4 are coherent with the differences found in the CH_4 emissions from these reservoirs in the stratification and mixing periods (León-Palmero et al., 2020). The wide range in CH_4 concentrations found in this study covers from values reported in temperate lakes (Donis et al., 2017; Grossart et al., 2011; Tang et al., 2014; West et al., 2016), to those found in tropical lakes and reservoirs (Murase et al., 2003; Naqvi et al., 2018; Okuku et al., 2019; Roland et al., 2017). In the surface mixing layer during the stratification period (i.e., epilimnion), we found values from 0.06 to 8.18 µM (Table S1), which is about eighty times the maximum values found in the surface waters of Lake Kivu (Africa) by Roland et al., (2017) and similar to the concentrations reported in subtropical and tropical reservoirs (Musenze et al. 2014, and references therein).

The dissolved CH_4 profiles showed considerable differences among depths during the summer stratification (Figs. 2a-4a, Figs S1a-9a, but were very homogeneous during the winter mixing in all the reservoirs (Figs. 2b-4b, Figs S1b-9b) (Table S1). Based on the differences found during the stratification period in the dissolved CH_4 profiles, we sorted the reservoirs in three types. The first type of CH_4 profile included six reservoirs that were characterized by an increase of the dissolved CH_4 from the oxycline to the anoxic bottom, just above the sediments, where CH_4 concentration reached its maximum. In these reservoirs, the oxycline may be spatially coupled to the thermocline, or not. When the oxycline and the thermocline were spatially coupled, the dissolved CH_4 concentration increased exponentially from the thermocline along the anoxic hypolimnion to the sediments. The reservoirs Béznar, San Clemente, and Iznájar showed this type of profile (Fig. 2a and Figs. S1a and S2a). The existence of a sizeable almost anoxic hypolimnion led to a massive accumulation of CH_4 in this layer. The differences in the CH_4 concentration between the surface and bottom waters were up to three orders of magnitude, as we found in Béznar (from the 0.25 to 56.17 µM; Fig. 2a), San Clemente (from the 0.23 to 45.15 µM; Fig S1a), and Iznájar (from the 0.82 µM to 213.64 µM; Fig. S2a). When the oxycline and the thermocline were not spatially coupled, the dissolved CH_4 concentration increased just above the sediments where the anoxic-oxic interface was near to the bottom. The reservoirs

Cubillas, La Bolera, and Francisco Abellán showed this profile type (Figs. S3a, S4a, and S5a). This accumulation of CH_4 in the hypolimnion and above sediments might be related to the high rates of methanogenesis in the sediments and its subsequent diffusion to the water column. Dissolved CH_4 concentration declines at the oxycline level, where the highest rates of CH_4 oxidation usually occur (Oswald et al., 2015, 2016). The CH_4 profiles in this group were similar to the ones found in tropical eutrophic and temperate reservoirs (Naqvi et al., 2018; West et al., 2016). The second profile type presents a small peak of metalimnetic CH_4, concomitant with peaks of dissolved oxygen, chlorophyll-a, photosynthetic picoeukaryotes, and cyanobacteria (Fig. 3a). In the Negratín reservoir, we found the maximum concentration of CH_4 in the oxic hypolimnion. Unlike several previous works in lakes (Blees et al., 2015; Grossart et al., 2011; Khatun et al., 2019; Murase et al., 2003), we did not find a metalimnetic CH_4 maximum. Khatun et al., (2019) described the existence of a metalimnetic CH_4 maximum in ten out of 14 lakes. The metalimnetic CH_4 maximum may represent a physically driven CH_4 accumulation due to solubility differences with the temperature at the thermocline, the epilimnetic CH_4 losses by emission, and the lateral inputs from the littoral zone (Donis et al., 2017; Encinas Fernández et al., 2016; Hofmann et al., 2010). The metalimnetic CH_4 maximum can also be determined by biological factors including the light inhibition of the methane oxidation (Murase and Sugimoto, 2005; Tang et al., 2014) or the distinctive methane production by phytoplankton due to availability of nutrients, light or precursors at this layer (Khatun et al., 2019). The third profile type included five reservoirs, in which the dissolved CH_4 profile presented a CH_4 accumulation more significant in the epilimnion than in the hypolimnion. The reservoirs Jándula, Bermejales, Rules, El Portillo, and Colomera showed this profile type (Fig. 4a, Figs. S6a–9a). These reservoirs had a mean CH_4 concentration in the water column significantly lower than the reservoirs from the first type. Similar profiles have been reported in temperate (Tang et al., 2014) and tropical lakes (Murase et al., 2003).

3. 2. CH_4 sources in the water column

We found two well-differentiated groups of CH_4 data sorted by the dissolved oxygen (D.O.) concentration (Fig. S10), like in previous studies (Tang et al., 2014). The first dataset included the samples with a D.O. lower than 7.5 μM (n = 18, hereafter anoxic samples). These samples belong to the hypolimnion of the study reservoirs during the stratification period. The second dataset included the samples with D.O. higher than 7.5 μM (n = 160, hereafter oxic samples). All the samples from the mixing period (n = 82) and most of the samples from the stratification period (n = 78) belong to this second dataset. We found significant differences (W = 2632, p-value < 0.001) between the concentration of CH_4 in the anoxic samples (median = 15.79 μM, min = 0.35 μM, max = 213.64 μM) and in the oxic samples (median = 0.15 μM, min = 0.02 μM, max = 8.17 μM). Since these two groups of samples are different, we determined their sources and drivers separately (Table S2).

3. 2. 1. CH_4 sources in anoxic waters

Archaeal methanogens are obligate anaerobes that decompose the organic matter and produce CH_4 in anoxic environments, as freshwater sediments. We analyzed the presence of the methanogenic *Archaea* in the anoxic samples of the water column

by targeting the gene *mcrA*. From the 77 samples selected for genetic analysis, twelve of them were anoxic. We did not detect the amplification of the *mcrA* gene in the PCR or the qPCR analysis in these twelve samples. Therefore, we assumed that the methanogenic *Archaea* were not present, as free-living microorganisms, in the water column of the anoxic samples. However, they may still be present in micro-anoxic zones in the water column (i.e., in the guts of zooplankton or within exopolymeric particles). Methanogenesis is a microbial process particularly sensitive to temperature (Marotta et al., 2014; Sepulveda-Jauregui et al., 2018; Yvon-Durocher et al., 2014). However, we did not find a significant relationship between the water temperature and the dissolved CH_4 concentration in the anoxic samples (n=17, p-value = 0.66). The no detection of the *mcrA* gene in the hypolimnetic waters and the absence of a relationship between the dissolved CH_4 and water temperature suggest that CH_4 production is not happening in the water column of the study reservoirs. We think that most methanogenic archaea must be present in the sediments, where they produce CH_4 that diffuses up to the water column producing vast accumulations of CH_4 in the hypolimnion.

Methanogenesis in the sediments may be affected by organic matter quantity and quality (West et al., 2012). Organic matter quantity is measured as the dissolved organic carbon concentration, whereas the organic matter quality usually is related to their phytoplanktonic vs terrestrial origin. In the study reservoirs, the dissolved organic carbon concentration did not show a significant relationship with the dissolved CH_4 concentration (n=12, p-value = 0.10, Table S2). We examined the importance of the autochthonous organic matter produced by primary producers using the total cumulative chlorophyll-a (Chl-a, mg m^{-2}). The cumulative Chl-a is considered as a surrogate for the vertical export of the phytoplankton biomass in the whole water column. We obtained that the CH_4 concentrations in anoxic samples was correlated to the cumulative Chl-a following a power function ($CH_4 = 3.0\ 10^{-4}$ Cumulative Chl-$a^{2.28}$; n=17, adj R^2=0.40, p-value <0.01, Table S2) (Fig. 5). The autochthonous organic matter appeared to be a better predictor for the concentration of CH_4 in anoxic waters than the dissolved organic matter concentration. In the study reservoirs, the dissolved organic carbon concentration was significantly related to the age of the reservoirs and the forestry coverage in their watersheds (León-Palmero et al., 2019). Therefore, in terms of quality, the total pool of dissolved organic carbon may be more representative of the allochthonous, recalcitrant and more resistant to microbial degradation carbon fraction. In contrast, the autochthonous organic matter may represent a more labile and biodegradable fraction. Previous experimental studies have demonstrated that the addition of algal biomass on sediment cores increase the CH_4 production more than the addition of terrestrial organic matter (Schwarz et al., 2008; West et al., 2012, 2015). The stimulation of the methanogenesis rates appears to be related to the lipid content in phytoplankton biomass (West et al. 2015). West et al. (2016) found a significant relationship between the chlorophyll-*a* concentration in the epilimnion and the potential methanogenesis rates from sediment incubations. In this study, we corroborate the importance of the autochthonous-derived organic matter determining the CH_4 concentrations in anoxic waters. Since we did not detect the existence of the *mcrA* gene in the water column, we considered that the production of methane by methanogenic *Archaea* occurred primarily in the sediments and was affected by the sedimentation of organic matter derived from phytoplankton.

3. 2. 2. CH_4 sources in oxic waters

In this study, the concentration of dissolved CH_4 ranged from 0.02 µM to 8.18 µM, and all the samples of the oxic waters were supersaturated with values always above 800% and ranging more than two orders of magnitude (Table S1). To determine the origin of this CH_4 supersaturation we examined the following potential sources: (1) the vertical and lateral CH_4 transport from deep layers and littoral zones, (2) the in situ CH_4 production by methanogenic *Archaea* potentially tolerant to oxygen or by the methyl-phosphonate degradation under severe P-limitation, and 3) the in situ CH_4 production by processes associated to the phytoplanktonic community.

Vertical and lateral CH_4-transport from anoxic sediments to oxic waters

Several previous works have pointed out that CH_4 supersaturation in oxic waters can be explained by the vertical transport from the bottom sediments, and the lateral inputs from the littoral zones that are in contact with shallow sediments where methanogenesis occurs (Bastviken et al., 2004; Encinas Fernández et al., 2016; Michmerhuizen et al., 1996). To test the importance of the lateral and vertical transport explaining the concentration of CH_4 in the oxic waters of the study reservoirs, we used two morphometric parameters: the mean depth (m) as a proxy for the vertical transport and the shallowness index as a proxy for the lateral transport. The dissolved CH_4 concentration was an exponential decay function of the reservoir mean depth (Fig. 6a) both during the stratification period ($CH_4 = 4.0\ 10^{-2}\ e^{(50.0/\ mean\ depth)}$, adj $R^2 = 0.95$) and during the mixing period ($CH_4 = 3.7\ 10^{-2}\ e^{(22.9/\ mean\ depth)}$, adj $R^2 = 0.54$) (Fig. 6a). We observed that in reservoirs with a mean depth shallower than 16 meters, the dissolved CH_4 concentration increased exponentially (Fig. 6a). Several studies have proposed that the vertical transport of CH_4 from bottom sediments explains the supersaturation in surface waters (Rudd & Hamilton 1978, Michmerhuizen et al. 1996, Murase et al. 2003, Bastviken et al. 2004). However, the vertical diffusion rates of dissolved gases across the thermocline are too low in deep and thermally stratified systems and no movements of methane upwards from the hypolimnion have been detected (Rudd and Hamilton, 1978). However, in shallow reservoirs, the hydrostatic pressure might be reduced promoting CH_4 diffusion from the anoxic layers.

The shallowness index increases in elongated and dendritic reservoirs with more impact of the littoral zone and decreases in near-circular reservoirs, with low shoreline length per surface. However, we did not find a significant relationship between the shallowness index and the dissolved CH_4 concentration (Fig. 6b). One explanation for the absence of this relationship could be the relatively large size of the reservoirs. Although the reservoir size covered more than one order of magnitude (Table 1), all reservoirs have a size larger than 1 Km^2. Previous studies have shown that CH_4 lateral diffusion may be an important process in areas near to the littoral zone and small lakes. Hofmann et al., (2010) found higher concentrations in the shallow littoral zones than in the open waters. DelSontro et al., (2018) predicted that lateral inputs from littoral zones to pelagic waters are more critical in small and round lakes than in large and elongated lakes. Nevertheless, the differences between the observations and predictions from the model suggested that these lateral inputs may not be enough

to explain CH_4 concentration in open waters, where in situ production may prevail over lateral transport (DelSontro et al., 2018).

In situ CH_4-production by methanogenic *Archaea* or methyl-phosphonate degradation

The ubiquitous CH_4 supersaturation found in oxic waters appear not to be fully explained by the vertical and lateral transport underlining that there is an in situ production of CH_4 as proposed by Bogard et al., (2014), DelSontro et al., (2018), and Grossart et al., (2011). We studied the presence of the methanogenic *Archaea* in the oxic samples by targeting the gene *mcrA*, but we were unable to detect this gene (Fig. S11). This result indicates that methanogenic *Archaea* were not present, at least as free-living microorganisms, in a significant number in the water column of the oxic samples. The classical methanogens (i.e., *Archaea* with the *mcrA* gene) are obligate anaerobes without the capacity to survive and produce CH_4 under aerobic conditions (Chistoserdova et al., 1998). Previous studies by Angel et al., (2011) and Angle et al., (2017) showed that methanogens might tolerate oxygen exposure in soils and Grossart et al., (2011) detected potential methanogenic *Archaea* attached to photoautotrophs in lake oxic waters. Unfortunately, we did not test their occurrence in large particles, phytoplankton or zooplankton guts, although some authors have detected them in these microsites particles (Angelis and Lee, 1994; Karl and Tilbrook, 1994).

We also considered the possibility of methylphosphonates degradation as an in situ CH_4 source. This metabolic pathway appears in the bacterioplankton under chronic starvation for phosphorus (Karl et al., 2008). Several pieces of evidence have shown that marine bacterioplankton can degrade the MPn and produce CH_4 through the C–P lyase activity in typically phosphorus starved environments, as the ocean gyres (Beversdorf et al., 2010; Carini et al., 2014; Repeta et al., 2016; Teikari et al., 2018; del Valle and Karl, 2014). Freshwater bacteria can also degrade the MPn and produce CH_4, as it has been demonstrated in Lake Matano (Yao et al., 2016b, 2016a). Lake Matano is an ultra-oligotrophic lake with a severe P deficiency (below 0.050 μmol P L^{-1}) due to the permanent stratification, iron content, and extremely low nutrient inputs (Crowe et al., 2008; Sabo et al., 2008). The ratio of dissolved inorganic nitrogen (DIN) to total phosphorus (TP) (μmol N: μmol P) is widely used to evaluate P-limitation (Morris and Lewis, 1988). DIN:TP ratios greater than 4 are indicative of phosphorus limitation (Axler et al., 1994). In the study reservoirs, the TP concentration ranged from 0.13 to 1.85 μmol P L^{-1} during the stratification period, and from 0.10 to 2.17 μmol P L^{-1} during the mixing period. The DIN:TP ratio ranged from 15 to 985 during the stratification period, and from 28 to 690 during the mixing period. The more severe the P-limitation conditions, the higher the CH_4 production by methylphosphonates degradation is. However, we did not find a significant relationship between the DIN:TP ratio and the CH_4 concentration (Fig. 7). We also analyzed the presence and abundance of the gene *phnJ*, which encodes the enzyme complex C–P lyase that hydrolyzes the MPn and changes in response to phosphate availability. We did not detect the *phnJ* gene in the PCR or the qPCR analysis in any of the study samples (Fig. S12). These results indicate that the MPn degradation was not a quantitatively relevant source of CH_4 in the oxic waters of the study reservoirs. Our results are in concordance with Grossart et al. (2011), who did not detect CH_4 production by adding inorganic

phosphate or methylphosphonates to lake samples in laboratory experiments. Although we used different methodologies, both studies may indicate that MPn degradation is only an important source of CH_4 in ultra-oligotrophic systems, as Lake Matano or ocean gyres.

In situ CH_4-production coupled to photosynthetic organisms

In the study reservoirs, we analyzed the relationship between photosynthetic organisms and the dissolved CH_4 concentration using the gross primary production (GPP, g O_2 m^{-3} d^{-1}), net ecosystem production (NEP, g O_2 m^{-3} d^{-1}), the concentration of chlorophyll-a (Chl-a, µg L^{-1}), and the abundance of photosynthetic picoeukaryotes (PPEs, cell mL^{-1}) and cyanobacteria (CYA, cell mL^{-1}). We determined GPP and NEP just once per reservoir during the stratification period (i.e., n=12).

The PPEs are essential components of the marine and freshwater phytoplankton, and they are eukaryotes with a size of 3.0 µm or less. In the freshwaters, the PPEs include species from different phyla, as unicellular *Chlorophyta* (green algae), and *Haptophyta*. Using optical microscopy, we determined the main groups of photosynthetic picoeukaryotes in the study reservoirs. PPEs were non-colonial green algae from the order *Chlorococcales* (class *Chlorophyceae,* phylum *Chlorophyta),* and the genus *Chrysochromulina* spp., (class *Coccolithophyceae,* phylum *Haptophyta*). The cyanobacteria detected were mainly phycoerythrin-rich picocyanobacteria, although we also detected phycocyanin-rich picocyanobacteria in one reservoir (Béznar). We show the vertical profiles of the Chl-a concentration and the abundance of PPEs and CYA profiles of each reservoir in Figs. 2-4 and Figs. S1-S9. We also report the minimum, the quartiles, and the maximum values for the Chl-a concentration and the abundance of PPEs and CYA during the stratification and the mixing periods in Table S2. The abundance of cyanobacteria ranged from 1.51 x10^3 to 2.04 x 10^5 cells mL^{-1} and was more than one order of magnitude higher than the abundance of PPEs that ranged from 32 to 7.45 x10^3 cells mL^{-1}.

We found that the relationship between the gross primary production and the dissolved CH_4 concentration was only marginally significant (p-value = 0.077, n = 12) and not significant with the net ecosystem production (Table 3). The Chl-*a* concentration showed a significant relationship with the GPP (p-value < 0.01, n = 12, adj R^2 = 0.55), but the abundance of cyanobacteria or the abundance of the photosynthetic picoeukaryotes did not show a significant relationship with the GPP (p-value = 0.911, n = 12; p-value = 0.203, n = 12, respectively). We found significant power relationships between the Chl-a concentration, the abundance of photosynthetic picoeukaryotes, and the abundance of cyanobacteria with the concentration of dissolved CH_4 during the stratification period (Fig. 8a, 8b, and 8c respectively, and Table 3). During the mixing period, the only significant predictor of the dissolved CH_4 concentration was the abundance of photosynthetic picoeukaryotes (Fig. 8b). The variance explained, and the slope of the relationship (i.e. the exponent in the power relationship) between the dissolved CH_4 and the abundance of photosynthetic picoeukaryotes was higher during the stratification than during the mixing (Table 3). By comparing the stratification slopes, the effect per cell of PPEs on CH_4 concentration was slightly higher than the impact of cyanobacteria (Table 3). These results agree with previous studies that showed a closed link between the CH_4 concentration and the photosynthetic organisms, primary production, or chlorophyll-a concentration (Bogard et al., 2014; Grossart et al., 2011; Schmidt and Conrad, 1993; Tang et al., 2014). In this study, we show that the

PPEs abundance was a better predictor of the CH_4 concentration than the abundance of cyanobacteria. In the study reservoirs, the PPEs group included members from green algae and *Haptophyta*, which are regular components of the marine plankton. Therefore, these results may be relevant also for marine waters. Cyanobacteria have received more attention as potential producers of CH_4 in oxic conditions than photosynthetic picoeukaryotes (Berg et al., 2014; Bižić et al., 2020; Teikari et al., 2018). Klintzsch et al., (2019) demonstrated that widespread marine and freshwater haptophytes as *Emiliana huxleyi*, *Phaeocystis globosa* and *Chrysochromulina sp.* produce CH_4 under oxic conditions. They also observed that the cell abundances were significantly related to the amount of CH_4 produced. Interestingly, *Chrysochromulina* was one of the genera of PPEs that we detected in the study reservoirs. Grossart et al. (2011) also found CH_4 production in laboratory cultures of cyanobacteria and green algae.

Overall, these results indicate a clear association between the CH_4 production and the photosynthetic organisms from both *Eukarya* (picoeukaryotes) and *Bacteria* (cyanobacteria) domains. The pathways involved in the CH_4 production may be related to the central photosynthetic metabolism or the release of methylated by-products different from methylphosphonates during the photosynthesis. Previous studies demonstrated the CH_4 production in laboratory cultures using ^{13}C-labeled bicarbonate in haptophytes (Klintzsch et al., 2019; Lenhart et al., 2016), in marine, freshwater, and terrestrial cyanobacteria (Bižić et al., 2020), and major groups of phytoplankton (Hartmann et al., 2020). In these studies, the photosynthetic organisms uptake bicarbonate in the reductive pentose phosphate cycle (Calvin-Benson cycle) (Berg, 2011; Burns and Beardall, 1987). Therefore, CH_4 production may be a common pathway in the central metabolism of photosynthesis of all the cyanobacteria and algae in freshwaters and marine environments.

On the other hand, the production of CH_4 can also be related to the production of methylated compounds during photosynthesis. Lenhart et al. (2016) and Klintzsch et al., (2019) also detected the CH_4 production in cultures from the sulfur-bound methyl group of the methionine and methyl thioethers. Common substances as methionine can act as a methyl-group donor during the CH_4 production in plants and fungi (Lenhart et al. 2012, 2015). Besides, algae use part of the methionine for the synthesis of dimethylsulfoniopropionate (DMSP), an abundant osmolyte, the precursor of dimethyl sulfide (DMS), and dimethylsulphoxide (DMSO). These methylated substances produce methane during their degradation (Damm et al., 2008, 2010, 2015; Zindler et al., 2013). Bižić-Ionescu et al., (2018) also suggested that CH_4 could be produced from methylated amines under oxic conditions. These substances, together with other organosulphur compounds, can also produce CH_4 abiotically (Althoff et al., 2014; Bižić-Ionescu et al., 2018). The production of DMSP, DMS, and other methylated substances as isoprene, has been extensively studied in marine phytoplankton, showing that taxa as photosynthetic picoeukaryotes and the cyanobacteria are relevant sources (Shaw et al., 2003; Yoch, 2002). Recent studies have also reported that freshwater algae and cyanobacteria also produced DMS and isoprene (Steinke et al., 2018). Further studies are needed to quantify the potential role of all these methylated by-products as potential CH_4 sources quantitatively relevant in freshwaters.

3. 2. 3. Modeling the CH_4 production in oxic waters

The explanation of the CH_4 supersaturation in oxic waters in relatively large systems rely on the interaction of several processes as the transport from anoxic environments and the biological activity (DelSontro et al., 2018). In this study, we found that vertical transport (mean depth as surrogate), water temperature, and the abundance of photosynthetic picoeukaryotes and cyanobacteria had a significant effect on the dissolved CH_4 concentration. We combined these explanatory variables with significant effects using generalized additive models (GAMs). The GAM model for the stratification period (n=78) had a fit deviance of 82.7% and an explained variance (adj R^2) of 81.4 % (Table S3). The explanatory variables, in decreasing order, were: the photosynthetic picoeukaryotes abundance (log_{10} PPEs), the reservoir mean depth, the cyanobacteria abundance (log_{10} CYA), and the water temperature (Fig. 9a). The function obtained was: $Log_{10}\ CH_4 = -4.05 + 3.4\ 10^{-1}\ Log_{10}$ PPEs + $e^{(6.7/\ \text{mean depth})} + 1.7\ 10^{-1}\ Log_{10}$ CYA + $2.7\ 10^{-2}$ Temperature. The abundance of PPEs was the variable explaining most of the variance of dissolved CH_4 concentration ($Log_{10} CH_4$) during the stratification period, with an effect higher than the cyanobacteria abundance. The panels b to e in Fig. 9 show the partial responses of each explanatory variable.

The GAM model for the mixing period (n=82) only included two explanatory variables: the reservoir mean depth and the abundance of the photosynthetic picoeukaryotes. The reservoir mean depth was the variable explaining most of the variance of the dissolved CH_4 concentration ($Log_{10} CH_4$) during the mixing period, closely followed by the abundance of PPEs (Fig. 10a). We observed that the function of the effect of the mean depth on the CH_4 concentration changed between the two periods (Fig. 9c and Fig 10b). The function was more linear during the mixing period than during the stratification period likely because the mixed water column enabled the more uniform distribution of the CH_4 produced in the sediment, while the thermocline acted as a barrier to the diffusion during the stratification period. The model function for the mixing period was: $Log_{10}\ CH_4 = -2.07 + 1.5\ e^{(-0.04\ \text{mean depth})} + 1.8\ \ 10^{-1}\ Log_{10}$ PPEs, with a fit deviance of 53.9 % and an explained variance (adj R^2) of 52.1 % (Table S3). In Figure 10b and 10c, we show the partial response plots for these two variables. The results show that the abundance of photosynthetic picoeukaryotes can be key for explaining the dissolved CH_4 concentration in oxic waters, even though they have received less attention than cyanobacteria in previous studies (Berg et al., 2014; Bižić et al., 2020a; Teikari et al., 2018). Finally, we have also included a simple model to explain the dissolved CH_4 concentration ($Log_{10} CH_4$) using the data of both periods (n=160) and including widely used variables like the water temperature (ºC), mean depth (m), and chlorophyll-a concentration (Chl-a, µg L^{-1}) for future comparisons. The function of this model is: $Log_{10}\ CH_4 = -3.02 + 0.05$ Temperature + $e^{(7.72/\ \text{mean depth})} + Log_{10}$ (log10 Chl-a) +1)/ 11.71. This GAM model had a fit deviance of 69.3 % and an explained variance (adj R^2) of 68 % (Table S3).

Overall, during the stratification period, the in situ CH_4 production was coupled to the abundance of photosynthetic picoeukaryotes in oxic waters (Fig. 9a) and mean depths. This CH_4 source due to photosynthetic picoeukaryotes can be crucial in large, deep lakes and reservoirs, and the open ocean since the impact of the CH_4 transport from sediments (i.e., mean depth) decreases with increasing depths. In deeper reservoirs, the thermal stratification during the summer produced

that the vertical diffusion rates of CH_4 from sediments is limited. Rudd and Hamilton, (1978) did not detect any movement of CH_4 upwards from the hypolimnion during the stratification. Previous studies have suggested that the CH_4 produced in the oxic water column is the primary source of CH_4 in large and deep lakes (Bogard et al., 2014; DelSontro et al., 2018; Donis et al., 2017; Günthel et al., 2019). Günthel et al., (2019) shown that large lakes have a lower sediment area in comparison to the volume of the surface mixed layer than small lakes and that this fact determines the higher contribution of the oxic methane production to surface emission in large (>1 Km^2) lakes than in small ones. The photosynthetic picoeukaryotes identified in the study reservoirs are considered indicators of eutrophic conditions and they are bloom-forming genera (i.e., *Chlorococcales* and *Chrysochromulina* spp.) (Edvardsen and Paasche, 1998; Reynolds, 1984; Willén, 1987). Global future estimations suggest a rise in eutrophication and algal bloom over the next century due to climate change and the growing human population (Beaulieu et al., 2019). In that situation, photosynthetic picoeukaryotes as *Chlorococcales* and *Chrysochromulina* spp., and cyanobacteria, would lead to an increment in CH_4 production and emissions. Further studies are needed to understand better the role of the photosynthetic picoeukaryotes in the production of CH_4 in oxic waters, and to quantify their influence in the methane supersaturation and CH_4 fluxes from inland and oceanic waters.

4 Conclusions

The dissolved CH_4 concentration in the study reservoirs showed a considerable variability (i.e. up to four orders of magnitude) and presented a clear seasonality. Surface waters were always supersaturated in CH_4. The concentration of CH_4 was closely linked to the photosynthetic organisms. In the anoxic waters, the depth-cumulative chlorophyll-a concentration, a proxy for the phytoplanktonic biomass exported to sediments, determined the CH_4 concentration. In the oxic waters, we considered different potential CH_4 sources, including the vertical and lateral transport of CH_4 from anoxic zones and *in situ* production. The mean depth of the reservoirs, as a surrogate of the CH_4 transport from sediment to the oxic waters, contributed in shallow systems. We did not detect methanogenic *Archaea* or methylphosphonates degradation target genes (i.e. *mcrA* and *phnJ* genes, respectively), which suggests that these pathways are not responsible for the in situ production of CH_4 in the oxic waters of the study reservoirs. We found that dissolved CH_4 was coupled to the abundance of photosynthetic picoeukaryotes (PPEs) during both periods and to chlorophyll-a concentration and the abundance of and cyanobacteria during the stratification period. These PPEs were non-colonial green algae from the order *Chlorococcales* (class *Chlorophyceae,* phylum *Chlorophyta),* and the genus *Chrysochromulina* spp., (class *Coccolithophyceae,* phylum *Haptophyta*). Finally, we combined all the explanatory variables with significant effects and determined their relative contribution to the CH_4 concentration using generalized additive models (GAMs). The abundance of PPEs was the variable explaining most of the variance of dissolved CH_4 concentration during the stratification period, with an effect higher than the cyanobacteria abundance. During the mixing period, the reservoir mean depth and the abundance of the PPEs were the only drivers for CH_4 concentration. Our findings show that the abundance of PPEs can be relevant for explaining the dissolved

569 CH_4 concentration in oxic waters of large lakes and reservoirs.

570 **Data availability**

571 Additional figures and tables can be found in the supplementary information. The dataset associated with this manuscript
572 will be available at Pangaea: Dissolved concentrations of CH4, nutrients, and biological parameters in the water column of
573 twelve Mediterranean reservoirs in Southern Spain (https://doi.org/10.1594/PANGAEA.912535) and Primary production of
574 twelve Mediterranean reservoirs in Southern Spain (https://doi.org10.1594/PANGAEA.912555).

575 **Author contribution**

576 E.L.-P., R.M.-B. and I.R. contributed equally to this work. R.M.-B. and I.R. designed the study and obtained the funds. E.L.-
577 P., R.M.-B., and I.R. contributed to data acquisition during the reservoir samplings. E.L.-P. processed most of the chemical
578 and biological samples. A.C. performed the flow cytometry and part of the molecular analysis, and A.S. collaborated with
579 the dissolved CH_4 analysis using gas chromatography. E.L.-P., R.M.-B. and I.R. analyzed the data and discussed the results.
580 E.L.-P. wrote the first draft manuscript, which was complemented by significant contributions of R.M.-B. and I.R.

581 **Competing interests**

582 The authors declare that the research was conducted in the absence of any commercial or financial relationships that could be
583 construed as a potential conflict of interest.

584 **Acknowledgements**

585 This research was funded by the project HERA (CGL2014-52362-R) to IR and RM-B of the Spanish Ministry of Economy
586 and Competitiveness, the Modelling Nature Scientific Unit (UCE.PP2017.03) and the Consejería de Economía,
587 Conocimiento, Empresas y Universidad from Andalucia and European Regional Development Fund (ERDF), ref.
588 SOMM17/6109/UGR to IR. E.L-P and A. S. were supported by PhD fellowships from the Ministry of Education, Culture
589 and Sports (FPU014/02917 and FPU2014-04048, respectively). A. C-R. was supported by the Youth Employment Initiative
590 (YEI) from the Junta de Andalucía and financed by the European Commission (Ref 6017). We specially thank to Eulogio
591 Corral for the help in the field work and Dr. Jesús Forja, and Dra. Teodora Ortega for helping with gas chromatography
592 analysis at the University of Cádiz. We also thank to Dr. David Fernández Moreno from the Department of Botany at the
593 University of Granada for the taxonomical identification of the phytoplankton community.

References

Althoff, F., Benzing, K., Comba, P., McRoberts, C., Boyd, D. R., Greiner, S. and Keppler, F.: Abiotic methanogenesis from organosulphur compounds under ambient conditions, Nat. Commun., 5, 4205, doi:10.1038/ncomms5205, 2014.

Álvarez-Salgado, X. A. and Miller, A. E. J.: Simultaneous determination of dissolved organic carbon and total dissolved nitrogen in seawater by high temperature catalytic oxidation: conditions for precise shipboard measurements, Mar. Chem., 62(3), 325–333, doi:10.1016/S0304-4203(98)00037-1, 1998.

Angel, R., Matthies, D. and Conrad, R.: Activation of Methanogenesis in Arid Biological Soil Crusts Despite the Presence of Oxygen, PLOS ONE, 6(5), e20453, doi:10.1371/journal.pone.0020453, 2011.

Angelis, M. A. de and Lee, C.: Methane production during zooplankton grazing on marine phytoplankton, Limnol. Oceanogr., 39(6), 1298–1308, doi:10.4319/lo.1994.39.6.1298, 1994.

Angle, J. C., Morin, T. H., Solden, L. M., Narrowe, A. B., Smith, G. J., Borton, M. A., Rey-Sanchez, C., Daly, R. A., Mirfenderesgi, G., Hoyt, D. W., Riley, W. J., Miller, C. S., Bohrer, G. and Wrighton, K. C.: Methanogenesis in oxygenated soils is a substantial fraction of wetland methane emissions, Nat. Commun., 8, doi:10.1038/s41467-017-01753-4, 2017.

Aronow, S.: Shoreline development ratio, in Beaches and Coastal Geology, pp. 754–755, Springer US, Boston, MA., 1982.

Axler, R. P., Rose, C. and Tikkanen, C. A.: Phytoplankton Nutrient Deficiency as Related to Atmospheric Nitrogen Deposition in Northern Minnesota Acid-Sensitive Lakes, Can. J. Fish. Aquat. Sci., 51(6), 1281–1296, doi:10.1139/f94-128, 1994.

Baird, R. B., Eaton, A. D., Clesceri, L. S. and others: Standard methods for the examination of water and wastewater, edited by E. W. Rice, American Public Health Association Washington, DC., 2012.

Bastviken, D., Cole, J., Pace, M. and Tranvik, L.: Methane emissions from lakes: Dependence of lake characteristics, two regional assessments, and a global estimate, Glob. Biogeochem. Cycles, 18(4), 1–12, doi:10.1029/2004GB002238, 2004.

Bastviken, D., Tranvik, L. J., Downing, J. A., Crill, P. M. and Enrich-Prast, A.: Freshwater Methane Emissions Offset the Continental Carbon Sink, Science, 331(6013), 1–12, doi:10.1126/science.1196808, 2011.

Beaulieu, J. J., DelSontro, T. and Downing, J. A.: Eutrophication will increase methane emissions from lakes and impoundments during the 21st century, Nat. Commun., 10(1), 1375, doi:10.1038/s41467-019-09100-5, 2019.

Berg, A., Lindblad, P. and Svensson, B. H.: Cyanobacteria as a source of hydrogen for methane formation, World J. Microbiol. Biotechnol., 30(2), 539–545, doi:10.1007/s11274-013-1463-5, 2014.

Berg, I. A.: Ecological Aspects of the Distribution of Different Autotrophic CO_2 Fixation Pathways, Appl. Environ. Microbiol., 77(6), 1925–1936, doi:10.1128/AEM.02473-10, 2011.

Beversdorf, L. J., White, A. E., Björkman, K. M., Letelier, R. M. and Karl, D. M.: Phosphonate metabolism by Trichodesmium IMS101 and the production of greenhouse gases, Limnol. Oceanogr., 55(4), 1768–1778,

627 doi:10.4319/lo.2010.55.4.1768, 2010.
628 Bižić, M., Klintzsch, T., Ionescu, D., Hindiyeh, M. Y., Günthel, M., Muro-Pastor, A. M., Eckert, W., Urich, T., Keppler, F.
629 and Grossart, H.-P.: Aquatic and terrestrial cyanobacteria produce methane, Science Advances, 6(3), 9,
630 doi:10.1126/sciadv.aax5343, 2020a.
631 Bižić-Ionescu, M., Ionescu, D., Günthel, M., Tang, K. W., & Grossart, H. P. (2018). Oxic methane cycling: New evidence
632 for methane formation in Oxic lake water. *Biogenesis of Hydrocarbons, edited by: Stams, AJ M and Souna, DZ,*
633 *Springer International Publishing, Basel*, 1-22.
634 Blees, J., Niemann, H., Erne, M., Zopfi, J., Schubert, C. J. and Lehmann, M. F.: Spatial variations in surface water methane
635 super-saturation and emission in Lake Lugano, southern Switzerland, Aquat. Sci., 77(4), 535–545,
636 doi:10.1007/s00027-015-0401-z, 2015.
637 Bogard, M. J., del Giorgio, P. A., Boutet, L., Chaves, M. C. G., Prairie, Y. T., Merante, A. and Derry, A. M.: Oxic water
638 column methanogenesis as a major component of aquatic CH4 fluxes, Nat. Commun., 5, 5350,
639 doi:10.1038/ncomms6350, 2014.
640 Boström, K. H., Simu, K., Hagström, Å. and Riemann, L.: Optimization of DNA extraction for quantitative marine
641 bacterioplankton community analysis, Limnol. Oceanogr. Methods, 2(11), 365–373, doi:10.4319/lom.2004.2.365,
642 2004.
643 Burns, B. D. and Beardall, J.: Utilization of inorganic carbon by marine microalgae, J. Exp. Mar. Biol. Ecol., 107(1), 75–86,
644 doi:10.1016/0022-0981(87)90125-0, 1987.
645 Carini, P., White, A. E., Campbell, E. O. and Giovannoni, S. J.: Methane production by phosphate-starved SAR11
646 chemoheterotrophic marine bacteria, Nat. Commun., 5, 4346, doi:10.1038/ncomms5346, 2014.
647 Cellamare, M., Rolland, A. and Jacquet, S.: Flow cytometry sorting of freshwater phytoplankton, J. Appl. Phycol., 22(1),
648 87–100, doi:10.1007/s10811-009-9439-4, 2010.
649 Chistoserdova, L., Vorholt, J. A., Thauer, R. K. and Lidstrom, M. E.: C1 Transfer Enzymes and Coenzymes Linking
650 Methylotrophic Bacteria and Methanogenic Archaea, Science, 281(5373), 99–102, doi:10.1126/science.281.5373.99,
651 1998.
652 Cole, J. J., Pace, M. L., Carpenter, S. R. and Kitchell, J. F.: Persistence of net heterotrophy in lakes during nutrient addition
653 and food web manipulations, Limnol. Oceanogr., 45(8), 1718–1730, doi:10.4319/lo.2000.45.8.1718, 2000.
654 Collier, J. L.: Flow Cytometry and the Single Cell in Phycology, J. Appl. Phycol., 36(4), 628–644, doi:10.1046/j.1529-
655 8817.2000.99215.x, 2000.
656 Corzo, A., Jimenez-Gomez, F., Gordillo, F., Garcia-Ruiz, R. and Niell, F.: Synechococcus and Prochlorococcus-like
657 populations detected by flow cytometry in a eutrophic reservoir in summer., J. Plankton Res., 21(8), 1575–1581,
658 doi:10.1093/plankt/21.8.1575, 1999.
659 Crowe, S. A., O'Neill, A. H., Katsev, S., Hehanussa, P., Haffner, G. D., Sundby, B., Mucci, A. and Fowle, D. A.: The
660 biogeochemistry of tropical lakes: A case study from Lake Matano, Indonesia, Limnol. Oceanogr., 53(1), 319–331,

doi:10.4319/lo.2008.53.1.0319, 2008.

Damm, E., Kiene, R. P., Schwarz, J., Falck, E. and Dieckmann, G.: Methane cycling in Arctic shelf water and its relationship with phytoplankton biomass and DMSP, Mar. Chem., 109(1–2), 45–59, doi:10.1016/j.marchem.2007.12.003, 2008.

Damm, E., Helmke, E., Thoms, S., Schauer, U., Nöthig, E., Bakker, K. and Kiene, R. P.: Methane production in aerobic oligotrophic surface water in the central Arctic Ocean, Biogeosciences, 7(3), 1099–1108, doi:10.5194/bg-7-1099-2010, 2010.

Damm, E., Thoms, S., Beszczynska-Möller, A., Nöthig, E. M. and Kattner, G.: Methane excess production in oxygen-rich polar water and a model of cellular conditions for this paradox, Polar Sci., 9(3), 327–334, doi:10.1016/j.polar.2015.05.001, 2015.

Deemer, B. R., Harrison, J. A., Li, S., Beaulieu, J. J., DelSontro, T., Barros, N., Bezerra-Neto, J. F., Powers, S. M., dos Santos, M. A. and Vonk, J. A.: Greenhouse Gas Emissions from Reservoir Water Surfaces: A New Global Synthesis, BioScience, 66(11), 949–964, doi:10.1093/biosci/biw117, 2016.

DelSontro, T., del Giorgio, P. A. and Prairie, Y. T.: No Longer a Paradox: The Interaction Between Physical Transport and Biological Processes Explains the Spatial Distribution of Surface Water Methane Within and Across Lakes, Ecosystems, 21(6), 1073–1087, doi:10.1007/s10021-017-0205-1, 2018.

Dlugokencky, E. J.: Trends in Atmospheric Methane. Globally averaged marine surface monthly mean data., NOAA/ESRL. [online] Available from: www.esrl.noaa.gov/gmd/ccgg/trends_ch4/, 2019.

Donis, D., Flury, S., Stöckli, A., Spangenberg, J. E., Vachon, D. and McGinnis, D. F.: Full-scale evaluation of methane production under oxic conditions in a mesotrophic lake, Nat. Commun., 8(1), 1661, doi:10.1038/s41467-017-01648-4, 2017.

Edvardsen, B. and Paasche, E.: Bloom dynamics and physiology of Prymnesium and Chrysochromulina, NATO ASI SERIES G ECOLOGICAL SCIENCES, 41, 193–208, 1998.

Encinas Fernández, J., Peeters, F. and Hofmann, H.: On the methane paradox: Transport from shallow water zones rather than in situ methanogenesis is the major source of CH_4 in the open surface water of lakes, JGR: Biogeosciences, 121(10), 2717–2726, doi:10.1002/2016JG003586, 2016.

Fox, A., Kwapinski, W., Griffiths, B. S. and Schmalenberger, A.: The role of sulfur- and phosphorus-mobilizing bacteria in biochar-induced growth promotion of Lolium perenne, FEMS Microbiol. Ecol., 90(1), 78–91, doi:10.1111/1574-6941.12374, 2014.

Fox, J. and Weisberg, S.: An R Companion to Applied Regression, Second., Sage, Thousand Oaks CA. [online] Available from: http://socserv.socsci.mcmaster.ca/jfox/Books/Companion, 2011.

Gasol, J. M. and Giorgio, P. A. del: Using flow cytometry for counting natural planktonic bacteria and understanding the structure of planktonic bacterial communities, Sci. Mar., 64(2), 197–224, doi:10.3989/scimar.2000.64n2197, 2000.

Gomez-Garcia, M. R., Davison, M., Blain-Hartnung, M., Grossman, A. R. and Bhaya, D.: Alternative pathways for phosphonate metabolism in thermophilic cyanobacteria from microbial mats, ISME J., 5(1), 141–149,

doi:10.1038/ismej.2010.96, 2011.

Grabarse, W., Mahlert, F., Duin, E. C., Goubeaud, M., Shima, S., Thauer, R. K., Lamzin, V. and Ermler, U.: On the mechanism of biological methane formation: structural evidence for conformational changes in methyl-coenzyme M reductase upon substrate binding, J. Mol. Biol., 309(1), 315–330, doi:10.1006/jmbi.2001.4647, 2001.

Gross, J. and Ligges, U.: nortest: Tests for Normality. [online] Available from: https://CRAN.R-project.org/package=nortest (Accessed 3 June 2018), 2015.

Grossart, H.-P., Frindte, K., Dziallas, C., Eckert, W. and Tang, K. W.: Microbial methane production in oxygenated water column of an oligotrophic lake, PNAS, 108(49), 19657–19661, doi:10.1073/pnas.1110716108, 2011.

Günthel, M., Donis, D., Kirillin, G., Ionescu, D., Bizic, M., McGinnis, D. F., Grossart, H.-P. and Tang, K. W.: Contribution of oxic methane production to surface methane emission in lakes and its global importance, Nat. Commun., 10(1), 1–10, doi:10.1038/s41467-019-13320-0, 2019.

Hartmann, J. F., Günthel, M., Klintzsch, T., Kirillin, G., Grossart, H.-P., Keppler, F. and Isenbeck-Schröter, M.: High Spatiotemporal Dynamics of Methane Production and Emission in Oxic Surface Water, Environ. Sci. Technol., 54(3), 1451–1463, doi:10.1021/acs.est.9b03182, 2020.

Hastie, T. and Tibshirani, R.: Generalized Additive Models, Statist. Sci., 1(3), 297–310, doi:10.1214/ss/1177013604, 1986.

Hastie, T. and Tibshirani, R. J.: Generalized additive models, London: Chapman and Hall., 1990.

Hofmann, H., Federwisch, L. and Peeters, F.: Wave-induced release of methane: Littoral zones as source of methane in lakes, Limnology and Oceanography, 55(5), 1990–2000, doi:10.4319/lo.2010.55.5.1990, 2010.

Jähne, B., Münnich, K. O., Bösinger, R., Dutzi, A., Huber, W. and Libner, P.: On the parameters influencing air-water gas exchange, J. Geophys. Res. Oceans, 92(C2), 1937–1949, doi:10.1029/JC092iC02p01937, 1987.

Jarrell, K. F.: Extreme Oxygen Sensitivity in Methanogenic Archaebacteria, BioScience, 35(5), 298–302, doi:10.2307/1309929, 1985.

Karl, D. M. and Tilbrook, B. D.: Production and transport of methane in oceanic particulate organic matter, Nature, 368(6473), 732–734, doi:10.1038/368732a0, 1994.

Karl, D. M., Beversdorf, L., Björkman, K. M., Church, M. J., Martinez, A. and Delong, E. F.: Aerobic production of methane in the sea, Nature Geosci., 1(7), 473–478, doi:10.1038/ngeo234, 2008.

Khatun, S., Iwata, T., Kojima, H., Fukui, M., Aoki, T., Mochizuki, S., Naito, A., Kobayashi, A. and Uzawa, R.: Aerobic methane production by planktonic microbes in lakes, Science of The Total Environment, 696, 133916, doi:10.1016/j.scitotenv.2019.133916, 2019.

Khatun, S., Iwata, T., Kojima, H., Ikarashi, Y., Yamanami, K., Imazawa, D., Kenta, T., Shinohara, R. and Saito, H.: Linking Stoichiometric Organic Carbon–Nitrogen Relationships to planktonic Cyanobacteria and Subsurface Methane Maximum in Deep Freshwater Lakes, Water, 12(2), 402, doi:10.3390/w12020402, 2020.

Kiene, R. P.: Production and consumption of methane in aquatic systems, Microbial Production and Consumption of Greenhouse Gases: Methane, Nitrogen Oxides, and Halomethanes, 1991.

729 Klintzsch, T., Langer, G., Nehrke, G., Wieland, A., Lenhart, K. and Keppler, F.: Methane production by three widespread
730 marine phytoplankton species: release rates, precursor compounds, and potential relevance for the environment,
731 Biogeosciences, 16(20), 4129–4144, doi:https://doi.org/10.5194/bg-16-4129-2019, 2019.
732 Lenhart, K., Bunge, M., Ratering, S., Neu, T. R., Schüttmann, I., Greule, M., Kammann, C., Schnell, S., Müller, C., Zorn, H.
733 and Keppler, F.: Evidence for methane production by saprotrophic fungi, Nat. Commun., 3, 1046,
734 doi:10.1038/ncomms2049, 2012.
735 Lenhart, K., Althoff, F., Greule, M. and Keppler, F.: Technical Note: Methionine, a precursor of methane in living plants,
736 Biogeosciences, 12(6), 1907–1914, doi:10.5194/bg-12-1907-2015, 2015.
737 Lenhart, K., Klintzsch, T., Langer, G., Nehrke, G., Bunge, M., Schnell, S. and Keppler, F.: Evidence for methane production
738 by the marine algae Emiliania huxleyi, Biogeosciences, 13(10), 3163–3174, doi:10.5194/bg-13-3163-2016, 2016.
739 León-Palmero, E., Reche, I. and Morales-Baquero, R.: Atenuación de luz en embalses del sur-este de la Península Ibérica,
740 Ingeniería del agua, 23(1), 65–75, doi:10.4995/ia.2019.10655, 2019.
741 León-Palmero, E., Morales-Baquero, R. and Reche, I.: Greenhouse gas fluxes from reservoirs determined by watershed
742 lithology, morphometry, and anthropogenic pressure, Environ. Res. Lett., 15(4), 044012, doi:10.1088/1748-
743 9326/ab7467, 2020.
744 Liu, H., Jing, H., Wong, T. H. C. and Chen, B.: Co-occurrence of phycocyanin- and phycoerythrin-rich Synechococcus in
745 subtropical estuarine and coastal waters of Hong Kong, Environ. Microbiol. Rep., 6(1), 90–99, doi:10.1111/1758-
746 2229.12111, 2014.
747 Marotta, H., Pinho, L., Gudasz, C., Bastviken, D., Tranvik, L. J. and Enrich-Prast, A.: Greenhouse gas production in low-
748 latitude lake sediments responds strongly to warming, Nature Clim. Change, 4(6), 467–470,
749 doi:10.1038/nclimate2222, 2014.
750 Michmerhuizen, C. M., Striegl, R. G. and McDonald, M. E.: Potential methane emission from north-temperate lakes
751 following ice melt, Limnol. Oceanogr., 41(5), 985–991, doi:10.4319/lo.1996.41.5.0985, 1996.
752 Mitsch, W. J., Bernal, B., Nahlik, A. M., Mander, Ü., Zhang, L., Anderson, C. J., Jørgensen, S. E. and Brix, H.: Wetlands,
753 carbon, and climate change, Landsc. Ecol., 28(4), 583–597, doi:10.1007/s10980-012-9758-8, 2012.
754 Morris, D. P. and Lewis, W. M.: Phytoplankton nutrient limitation in Colorado mountain lakes, Freshwater Biol., 20(3),
755 315–327, doi:10.1111/j.1365-2427.1988.tb00457.x, 1988.
756 Mortimer, C. H.: The oxygen content of air-saturated fresh waters, and aids in calculating percentage saturation,
757 Schweizerbart Science Publishers, Stuttgart, Germany. [online] Available from:
758 http://www.schweizerbart.de//publications/detail/isbn/9783510520060/Mitteilungen_IVL_Nr_6, 1956.
759 Murase, J. and Sugimoto, A.: Inhibitory effect of light on methane oxidation in the pelagic water column of a mesotrophic
760 lake (Lake Biwa, Japan), Limnology and Oceanography, 50(4), 1339–1343, doi:10.4319/lo.2005.50.4.1339, 2005.
761 Murase, J., Sakai, Y., Sugimoto, A., Okubo, K. and Sakamoto, M.: Sources of dissolved methane in Lake Biwa, Limnology,
762 4(2), 91–99, doi:10.1007/s10201-003-0095-0, 2003.

763 Murphy, J. and Riley, J. P.: A modified single solution method for the determination of phosphate in natural waters, Anal.
764 Chim. Acta, 27(Supplement C), 31–36, doi:10.1016/S0003-2670(00)88444-5, 1962.
765 Musenze, R. S., Grinham, A., Werner, U., Gale, D., Sturm, K., Udy, J. and Yuan, Z.: Assessing the spatial and temporal
766 variability of diffusive methane and nitrous oxide emissions from subtropical freshwater reservoirs, Environ. Sci.
767 Technol., 48(24), 14499–14507, doi:10.1021/es505324h, 2014.
768 Naqvi, S. W. A., Lam, P., Narvenkar, G., Sarkar, A., Naik, H., Pratihary, A., Shenoy, D. M., Gauns, M., Kurian, S., Damare,
769 S., Duret, M., Lavik, G. and Kuypers, M. M. M.: Methane stimulates massive nitrogen loss from freshwater reservoirs
770 in India, Nat. Commun., 9(1), 1–10, doi:10.1038/s41467-018-03607-z, 2018.
771 Odum, H. T.: Primary Production in Flowing Waters, Limnol. Oceanogr., 1(2), 102–117, doi:10.4319/lo.1956.1.2.0102,
772 1956.
773 Okuku, E. O., Bouillon, S., Tole, M. and Borges, A. V.: Diffusive emissions of methane and nitrous oxide from a cascade of
774 tropical hydropower reservoirs in Kenya, Lakes & Reservoirs: Research & Management, 24(2), 127–135,
775 doi:10.1111/lre.12264, 2019.
776 Oswald, K., Milucka, J., Brand, A., Littmann, S., Wehrli, B., Kuypers, M. M. M. and Schubert, C. J.: Light-Dependent
777 Aerobic Methane Oxidation Reduces Methane Emissions from Seasonally Stratified Lakes, PLOS ONE, 10(7),
778 doi:10.1371/journal.pone.0132574, 2015.
779 Oswald, K., Jegge, C., Tischer, J., Berg, J., Brand, A., Miracle, M. R., Soria, X., Vicente, E., Lehmann, M. F., Zopfi, J. and
780 Schubert, C. J.: Methanotrophy under Versatile Conditions in the Water Column of the Ferruginous Meromictic Lake
781 La Cruz (Spain), Front. Microbiol., 7, doi:10.3389/fmicb.2016.01762, 2016.
782 Owens, N. J. P., Law, C. S., Mantoura, R. F. C., Burkill, P. H. and Llewellyn, C. A.: Methane flux to the atmosphere from
783 the Arabian Sea, Nature, 354(6351), 293–296, doi:10.1038/354293a0, 1991.
784 Peeters, F., Wüest, A., Piepke, G. and Imboden, D. M.: Horizontal mixing in lakes, J. Geophys. Res. Oceans, 101(C8),
785 18361–18375, doi:10.1029/96JC01145, 1996.
786 Peeters, F., Fernandez Encinas, J. and Hofmann, H.: Sediment fluxes rather than oxic methanogenesis explain diffusive CH_4
787 emissions from lakes and reservoirs, Sci. Rep., 9(1), 1–10, doi:10.1038/s41598-018-36530-w, 2019.
788 R Core Team: R: A Language and Environment for Statistical Computing, R Foundation for Statistical Computing, Vienna,
789 Austria. [online] Available from: http://www.R-project.org/, 2014.
790 Rasilo, T., Prairie, Y. T. and del Giorgio, P. A.: Large-scale patterns in summer diffusive CH_4 fluxes across boreal lakes, and
791 contribution to diffusive C emissions, Glob. Change Biol., 21(3), 1124–1139, doi:10.1111/gcb.12741, 2015.
792 Repeta, D. J., Ferrón, S., Sosa, O. A., Johnson, C. G., Repeta, L. D., Acker, M., DeLong, E. F. and Karl, D. M.: Marine
793 methane paradox explained by bacterial degradation of dissolved organic matter, Nat. Geosci., 9(12), 884–887,
794 doi:10.1038/ngeo2837, 2016.
795 Reynolds, C. S.: Phytoplankton periodicity: the interactions of form, function and environmental variability, Freshwater
796 Biology, 14(2), 111–142, doi:10.1111/j.1365-2427.1984.tb00027.x, 1984.

797 Roland, F. A. E., Darchambeau, F., Morana, C. and Borges, A. V.: Nitrous oxide and methane seasonal variability in the
798 epilimnion of a large tropical meromictic lake (Lake Kivu, East-Africa), Aquat. Sci., 79(2), 209–218,
799 doi:10.1007/s00027-016-0491-2, 2017.
800 Rudd, J. W. M. and Hamilton, R. D.: Methane cycling in a eutrophic shield lake and its effects on whole lake metabolism,
801 Limnol. Oceanogr., 23(2), 337–348, doi:10.4319/lo.1978.23.2.0337, 1978.
802 Sabo, E., Roy, D., Hamilton, P. B., Hehanussa, P. E., McNeely, R. and Haffner, G. D.: The plankton community of Lake
803 Matano: factors regulating plankton composition and relative abundance in an ancient, tropical lake of Indonesia, in
804 Patterns and Processes of Speciation in Ancient Lakes, pp. 225–235, Springer., 2008.
805 Saunois, M., Bousquet, P., Poulter, B., Peregon, A., Ciais, P., Canadell, J. G., Dlugokencky, E. J., Etiope, G., Bastviken, D.,
806 Houweling, S., Janssens-Maenhout, G., Tubiello, F. N., Castaldi, S., Jackson, R. B., Alexe, M., Arora, V. K.,
807 Beerling, D. J., Bergamaschi, P., Blake, D. R., Brailsford, G., Brovkin, V., Bruhwiler, L., Crevoisier, C., Crill, P.,
808 Covey, K., Curry, C., Frankenberg, C., Gedney, N., Höglund-Isaksson, L., Ishizawa, M., Ito, A., Joos, F., Kim, H.-S.,
809 Kleinen, T., Krummel, P., Lamarque, J.-F., Langenfelds, R., Locatelli, R., Machida, T., Maksyutov, S., McDonald, K.
810 C., Marshall, J., Melton, J. R., Morino, I., Naik, V., O'Doherty, S., Parmentier, F.-J., Patra, P. K., Peng, C., Peng, S.,
811 Peters, G. P., Pison, I., Prigent, C., Prinn, R., Ramonet, M., Riley, W. J., Saito, M., Santini, M., Schroeder, R.,
812 Simpson, I. J., Spahni, R., Steele, P., Takizawa, A., Thornton, B. F., Tian, H., Tohjima, Y., Viovy, N., Voulgarakis,
813 A., van Weele, M., van der Werf, G. R., Weiss, R., Wiedinmyer, C., Wilton, D. J., Wiltshire, A., Worthy, D., Wunch,
814 D., Xu, X., Yoshida, Y., Zhang, B., Zhang, Z. and Zhu, Q.: The global methane budget 2000–2012, Earth Syst. Sci.
815 Data, 8, 697–751, 2016.
816 Schlesinger, W. H. and Bernhardt, E. S.: Biogeochemistry: An Analysis of Global Change, Academic Press., 2013.
817 Schmale, O., Wäge, J., Mohrholz, V., Wasmund, N., Gräwe, U., Rehder, G., Labrenz, M. and Loick-Wilde, N.: The
818 contribution of zooplankton to methane supersaturation in the oxygenated upper waters of the central Baltic Sea,
819 Limnol. Oceanogr., 63(1), 412–430, doi:10.1002/lno.10640, 2018.
820 Schmidt, U. and Conrad, R.: Hydrogen, carbon monoxide, and methane dynamics in Lake Constance, Limnol. Oceanogr.,
821 38(6), 1214–1226, doi:10.4319/lo.1993.38.6.1214, 1993.
822 Schubert, C. J. and Wehrli, B.: Contribution of Methane Formation and Methane Oxidation to Methane Emission from
823 Freshwater Systems, in Biogenesis of Hydrocarbons, edited by A. J. M. Stams and D. Sousa, pp. 1–31, Springer
824 International Publishing, Cham., 2018.
825 Schulz, M., Faber, E., Hollerbach, A., Schröder, H. G. and Güde, H.: The methane cycle in the epilimnion of Lake
826 Constance, Archiv für Hydrobiologie, 157–176, doi:10.1127/archiv-hydrobiol/151/2001/157, 2001.
827 Schwarz, J. I. K., Eckert, W. and Conrad, R.: Response of the methanogenic microbial community of a profundal lake
828 sediment (Lake Kinneret, Israel) to algal deposition, Limnol. Oceanogr., 53(1), 113–121,
829 doi:10.4319/lo.2008.53.1.0113, 2008.
830 Scranton, M. I. and Brewer, P. G.: Occurrence of methane in the near-surface waters of the western subtropical North-

Atlantic, Deep-Sea Res., 24(2), 127–138, doi:10.1016/0146-6291(77)90548-3, 1977.

Segers, R.: Methane production and methane consumption: a review of processes underlying wetland methane fluxes, Biogeochemistry, 41(1), 23–51, doi:10.1023/A:1005929032764, 1998.

Sepulveda-Jauregui, A., Hoyos-Santillan, J., Martinez-Cruz, K., Walter Anthony, K. M., Casper, P., Belmonte-Izquierdo, Y. and Thalasso, F.: Eutrophication exacerbates the impact of climate warming on lake methane emission, Sci. Total Environ., 636, 411–419, doi:10.1016/j.scitotenv.2018.04.283, 2018.

Seweryn, P., Van, L. B., Kjeldgaard, M., Russo, C. J., Passmore, L. A., Hove-Jensen, B., Jochimsen, B. and Brodersen, D. E.: Structural insights into the bacterial carbon-phosphorus lyase machinery, Nature, 525(7567), 68–72, doi:10.1038/nature14683, 2015.

Shaw, S. L., Chisholm, S. W. and Prinn, R. G.: Isoprene production by Prochlorococcus, a marine cyanobacterium, and other phytoplankton, Mar. Chem., 80(4), 227–245, doi:10.1016/S0304-4203(02)00101-9, 2003.

Sierra, A., Jiménez-López, D., Ortega, T., Ponce, R., Bellanco, M. J., Sánchez-Leal, R., Gómez-Parra, A. and Forja, J.: Spatial and seasonal variability of CH_4 in the eastern Gulf of Cadiz (SW Iberian Peninsula), Sci. Total Environ., 590–591, 695–707, doi:10.1016/j.scitotenv.2017.03.030, 2017.

Staehr, P. A., Bade, D., Bogert, M. C. V. de, Koch, G. R., Williamson, C., Hanson, P., Cole, J. J. and Kratz, T.: Lake metabolism and the diel oxygen technique: State of the science, Limnol. Oceanogr. Methods, 8(11), 628–644, doi:10.4319/lom.2010.8.0628, 2010.

Steinke, M., Hodapp, B., Subhan, R., Bell, T. G. and Martin-Creuzburg, D.: Flux of the biogenic volatiles isoprene and dimethyl sulfide from an oligotrophic lake, Sci. Rep., 8(1), 1–10, doi:10.1038/s41598-017-18923-5, 2018.

Tang, K. W., McGinnis, D. F., Frindte, K., Brüchert, V. and Grossart, H.-P.: Paradox reconsidered: Methane oversaturation in well-oxygenated lake waters, Limnol. Oceanogr., 59(1), 275–284, doi:10.4319/lo.2014.59.1.0275, 2014.

Tang, K. W., McGinnis, D. F., Ionescu, D. and Grossart, H.-P.: Methane Production in Oxic Lake Waters Potentially Increases Aquatic Methane Flux to Air, Environ. Sci. Technol. Lett., 3(6), 227–233, doi:10.1021/acs.estlett.6b00150, 2016.

Teikari, J. E., Fewer, D. P., Shrestha, R., Hou, S., Leikoski, N., Mäkelä, M., Simojoki, A., Hess, W. R. and Sivonen, K.: Strains of the toxic and bloom-forming Nodularia spumigena (cyanobacteria) can degrade methylphosphonate and release methane, ISME J., 12(6), 1619–1630, doi:10.1038/s41396-018-0056-6, 2018.

Thalasso, F., Sepulveda-Jauregui, A., Gandois, L., Martinez-Cruz, K., Gerardo-Nieto, O., Astorga-España, M. S., Teisserenc, R., Lavergne, C., Tananaev, N., Barret, M. and Cabrol, L.: Sub-oxycline methane oxidation can fully uptake CH_4 produced in sediments: case study of a lake in Siberia, Sci. Rep., 10(1), 1–7, doi:10.1038/s41598-020-60394-8, 2020.

Thanh-Duc, N., Crill, P. and Bastviken, D.: Implications of temperature and sediment characteristics on methane formation and oxidation in lake sediments, Biogeochemistry, 100(1), 185–196, doi:10.1007/s10533-010-9415-8, 2010.

Tilbrook, B. D. and Karl, D. M.: Methane sources, distributions and sinks from California coastal waters to the oligotrophic

North Pacific gyre, Mar. Chem., 49(1), 51–64, doi:10.1016/0304-4203(94)00058-L, 1995.

del Valle, D. A. and Karl, D. M.: Aerobic production of methane from dissolved water-column methylphosphonate and sinking particles in the North Pacific Subtropical Gyre, Aquat. Microb. Ecol., 73(2), 93–105, doi:10.3354/ame01714, 2014.

Wang, Q., Dore, J. E. and McDermott, T. R.: Methylphosphonate metabolism by Pseudomonas sp. populations contributes to the methane oversaturation paradox in an oxic freshwater lake, Environ. Microbiol., 19(6), 2366–2378, doi:10.1111/1462-2920.13747, 2017.

West, W. E., Coloso, J. J. and Jones, S. E.: Effects of algal and terrestrial carbon on methane production rates and methanogen community structure in a temperate lake sediment, Freshwater Biol., 57(5), 949–955, doi:10.1111/j.1365-2427.2012.02755.x, 2012.

West, W. E., McCarthy, S. M. and Jones, S. E.: Phytoplankton lipid content influences freshwater lake methanogenesis, Freshwater Biol., 60(11), 2261–2269, doi:10.1111/fwb.12652, 2015.

West, W. E., Creamer, K. P. and Jones, S. E.: Productivity and depth regulate lake contributions to atmospheric methane: Lake productivity fuels methane emissions, Limnol. Oceanogr., 61(S1), S51–S61, doi:10.1002/lno.10247, 2016.

White, A. K. and Metcalf, W. W.: Microbial Metabolism of Reduced Phosphorus Compounds, Annu. Rev. Microbiol., 61(1), 379–400, doi:10.1146/annurev.micro.61.080706.093357, 2007.

Wiesenburg, D. A. and Guinasso, N. L.: Equilibrium solubilities of methane, carbon monoxide, and hydrogen in water and sea water, J. Chem. Eng. Data, 24(4), 356–360, doi:10.1021/je60083a006, 1979.

Willén, E.: Phytoplankton and reversed Eutrophication in Lake Mälaren, Central Sweden, 1965–1983, Br. Phycol. J., 22(2), 193–208, doi:10.1080/00071618700650241, 1987.

Wood, S. N.: Generalized additive models: an introduction with R, Chapman and Hall/CRC, New York, USA., 2006.

Wood, S. N.: Fast stable restricted maximum likelihood and marginal likelihood estimation of semiparametric generalized linear models, J. R. Stat. Soc. Series B Stat. Methodol., 73(1), 3–36, doi:10.1111/j.1467-9868.2010.00749.x, 2011.

Yamamoto, S., Alcauskas, J. B. and Crozier, T. E.: Solubility of methane in distilled water and seawater, J. Chem. Eng. Data, 21(1), 78–80, doi:10.1021/je60068a029, 1976.

Yao, M., Henny, C. and Maresca, J. A.: Freshwater bacteria release methane as a byproduct of phosphorus acquisition, Appl. Environ. Microbiol., 82(23), 6994–7003, doi:10.1128/AEM.02399-16, 2016a.

Yao, M., Elling, F. J., Jones, C., Nomosatryo, S., Long, C. P., Crowe, S. A., Antoniewicz, M. R., Hinrichs, K.-U. and Maresca, J. A.: Heterotrophic bacteria from an extremely phosphate-poor lake have conditionally reduced phosphorus demand and utilize diverse sources of phosphorus, Environ. Microbiol., 18(2), 656–667, doi:10.1111/1462-2920.13063, 2016b.

Yoch, D. C.: Dimethylsulfoniopropionate: its sources, role in the marine food web, and biological degradation to dimethylsulfide, Appl. Environ. Microbiol., 68(12), 5804–5815, doi:10.1128/AEM.68.12.5804-5815.2002, 2002.

Yvon-Durocher, G., Allen, A. P., Bastviken, D., Conrad, R., Gudasz, C., St-Pierre, A., Thanh-Duc, N. and del Giorgio, P.

A.: Methane fluxes show consistent temperature dependence across microbial to ecosystem scales, Nature, 507(7493), 488–491, doi:10.1038/nature13164, 2014.

Zindler, C., Bracher, A., Marandino, C. A., Taylor, B., Torrecilla, E., Kock, A. and Bange, H. W.: Sulphur compounds, methane, and phytoplankton: interactions along a north–south transit in the western Pacific Ocean, Biogeosciences, 10(5), 3297–3311, doi:10.5194/bg-10-3297-2013, 2013.

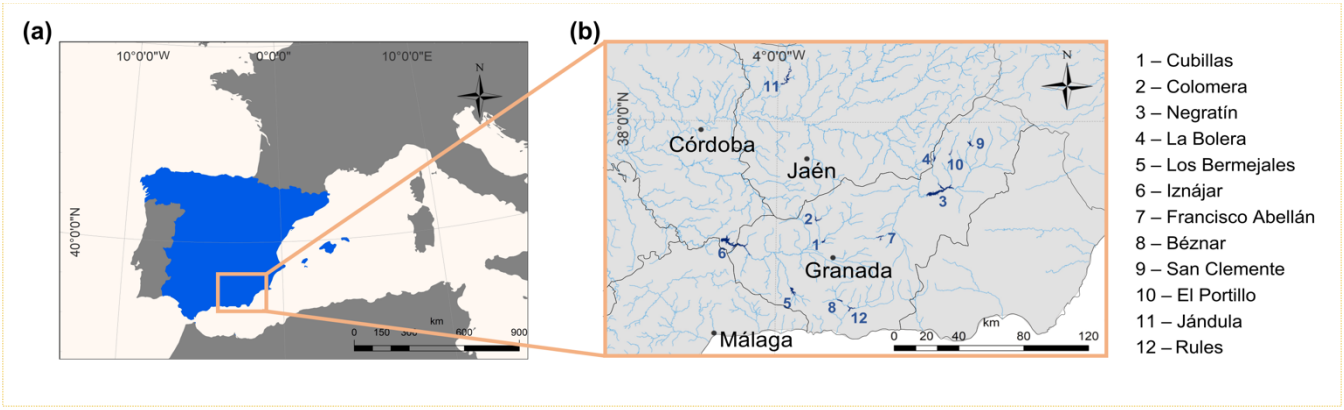

Figure 1: **Geographical location of the study reservoirs.** (**a**) The location area of the study reservoirs is delimited by an orange box in the South of the Iberian Peninsula. (**b**) Detailed location of the twelve reservoirs with the numbers (#1–12) and their corresponding names listed on the side. Geographical coordinates appear in Table 1. We obtained these maps using ArcGIS® 10.2 software (ESRI, 2012) under the Universidad de Granada license. ESRI: ArcGIS, Redlands, CA.

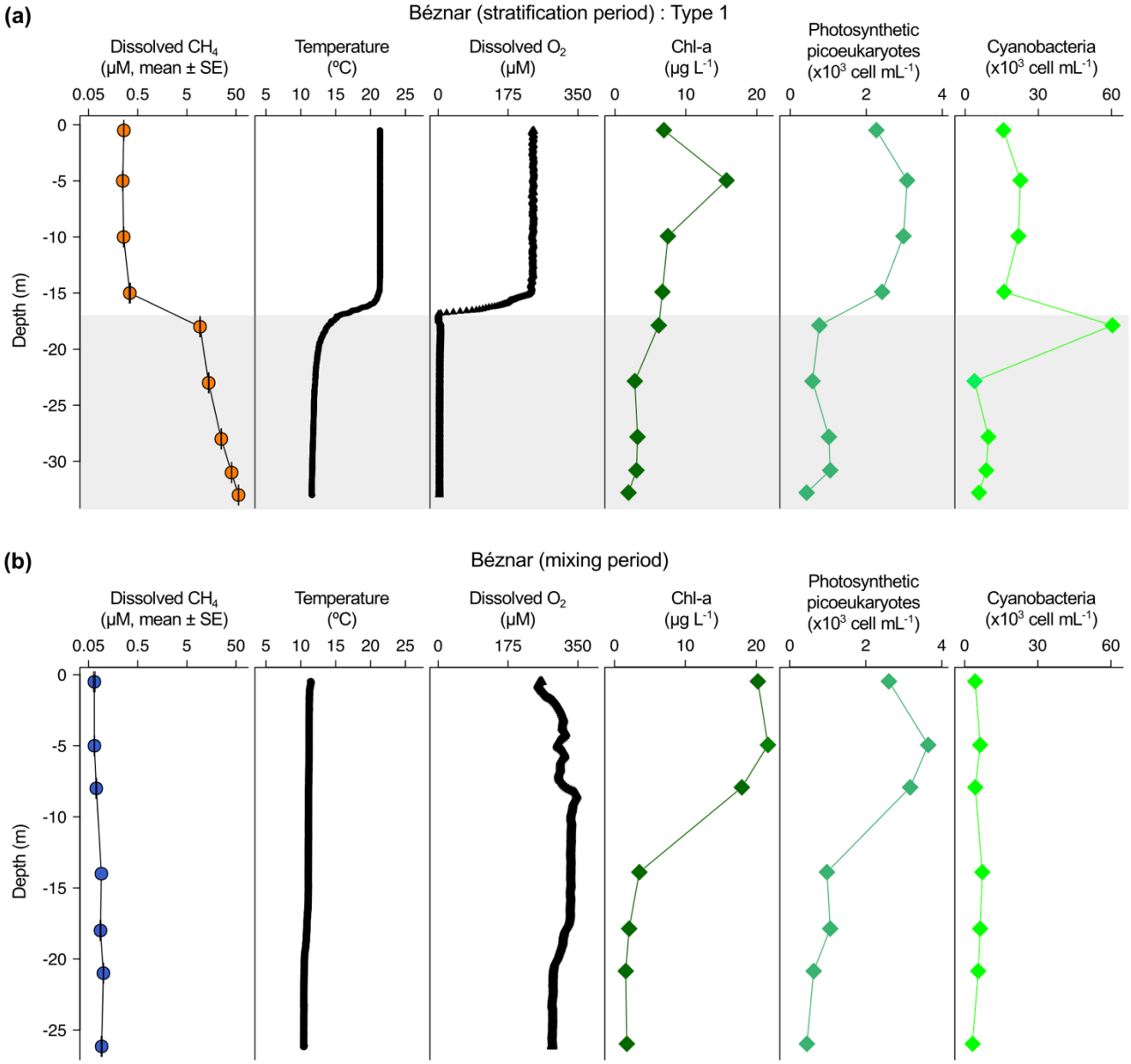

914

915 **Figure 2**: **Vertical profiles of physicochemical and biological variables in Béznar reservoir.** Dissolved methane concentration (CH_4,
916 µM), temperature (ºC), dissolved oxygen concentration (DO, µM), chlorophyll-a concentration (Chl-a, µg L^{-1}), abundance of
917 photosynthetic picoeukaryotes (cell mL^{-1}) and abundance of cyanobacteria (cell mL^{-1}) during the stratification period (**a**) and the mixing
918 period (**b**). The grey area represents the anoxic zone (DO < 7.5 µM). Note the logarithmic scales in the x-axis of the dissolved CH_4
919 profiles. The sampling for the stratification period was on October 7, 2016 and February 23, 2017 for the mixing period.

920

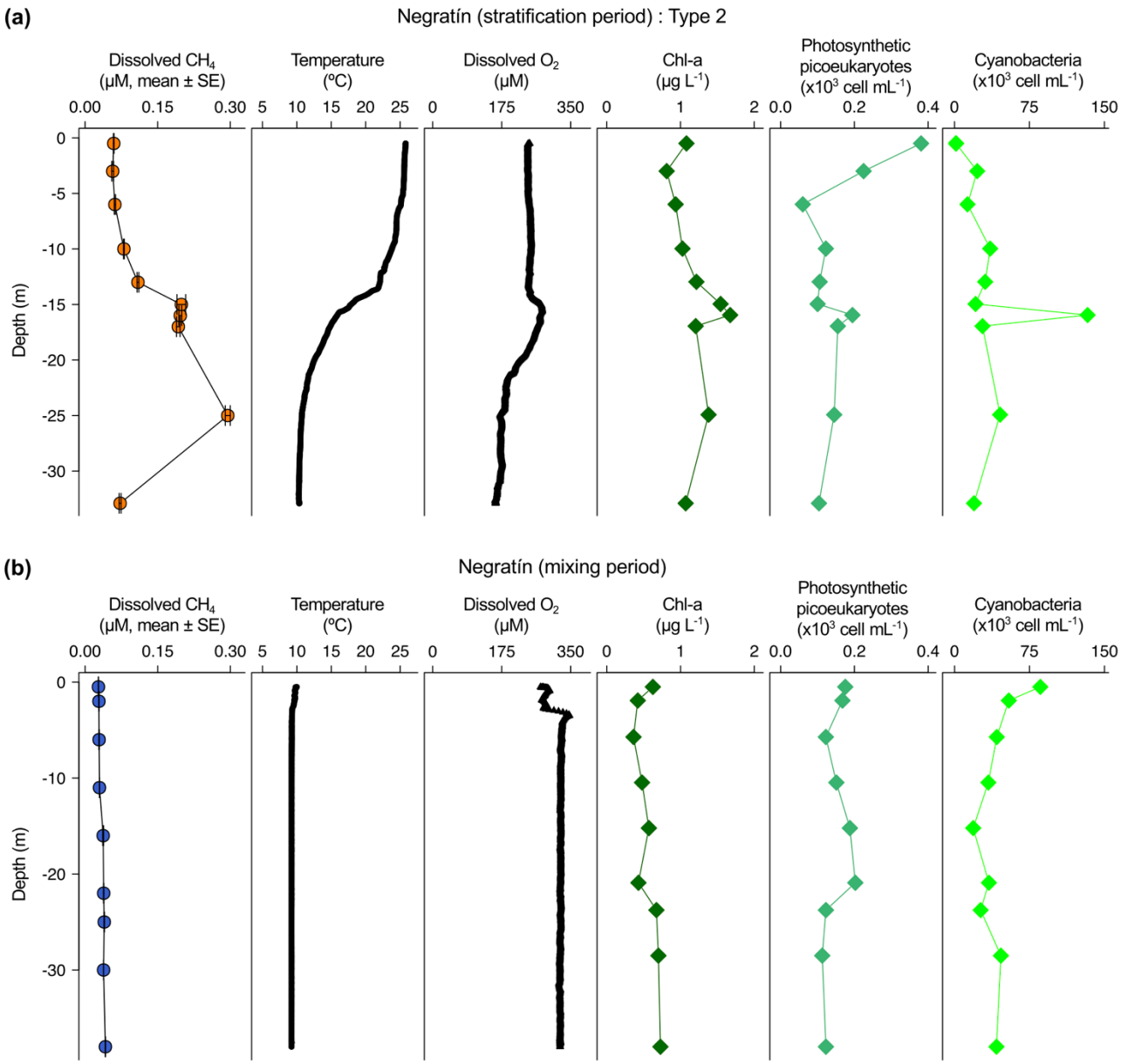

921

922 **Figure 3: Vertical profiles of physicochemical and biological variables in Negratín reservoir.** Dissolved methane concentration (CH_4,
923 µM), temperature (ºC), dissolved oxygen concentration (DO, µM), chlorophyll-a concentration (Chl-a, µg L^{-1}), abundance of
924 photosynthetic picoeukaryotes (cell mL^{-1}) and abundance of cyanobacteria (cell mL^{-1}) during the stratification period (**a**) and the mixing
925 period (**b**). The sampling for the stratification period was on July 27, 2016 and February 16, 2017 for the mixing period.

926

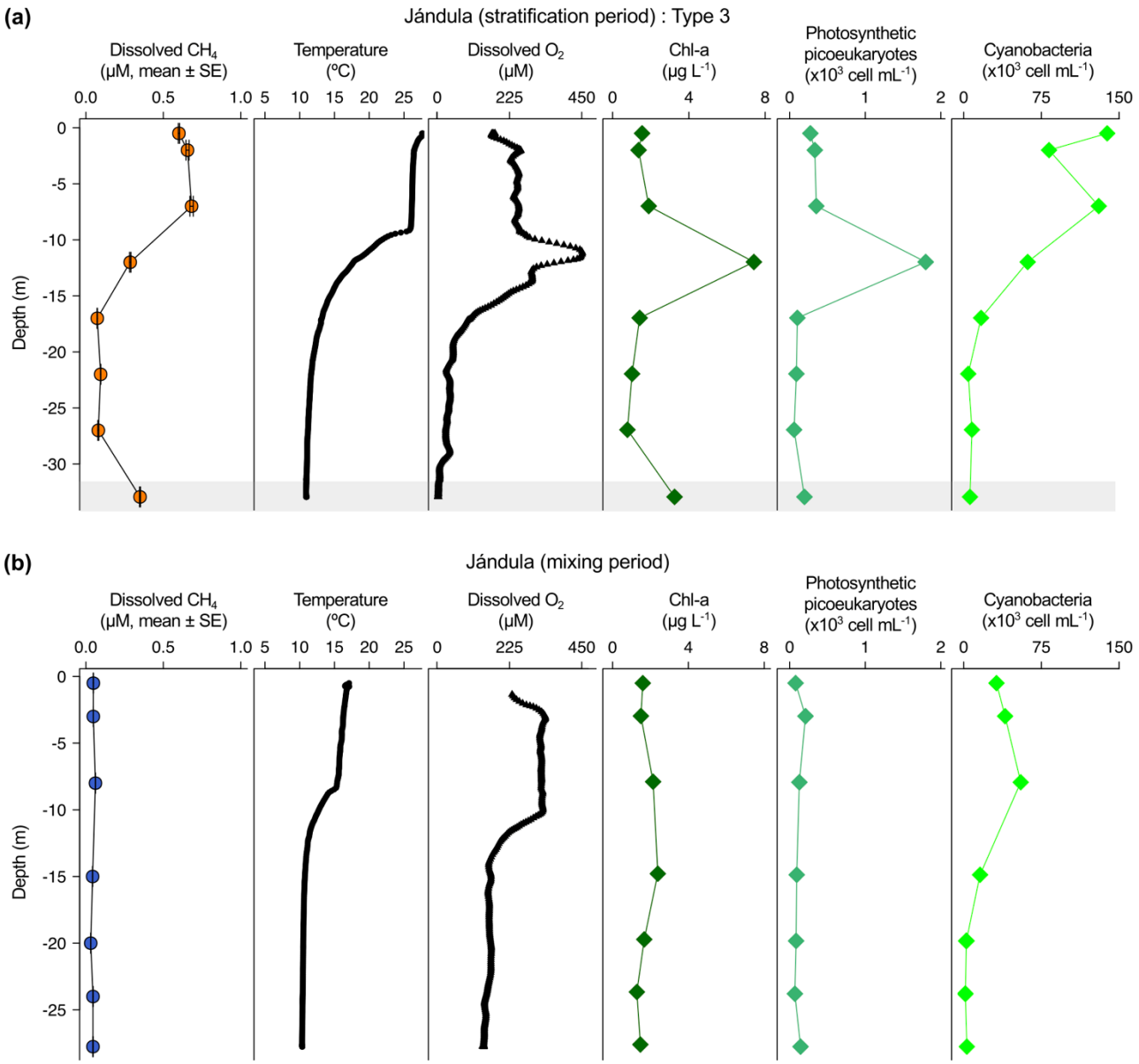

927

928 **Figure 4: Vertical profiles of physicochemical and biological variables in Jándula reservoir.** Dissolved methane concentration (CH_4,
929 µM), temperature (ºC), dissolved oxygen concentration (DO, µM), chlorophyll-a concentration (Chl-a, µg L^{-1}), abundance of
930 photosynthetic picoeukaryotes (cell mL^{-1}) and abundance of cyanobacteria (cell mL^{-1}) during the stratification period (**a**) and the mixing
931 period (**b**). The grey area represents the anoxic zone (DO < 7.5 µM). The sampling for the stratification period was on July 24, 2017 and
932 April 5, 2017 for the mixing period.

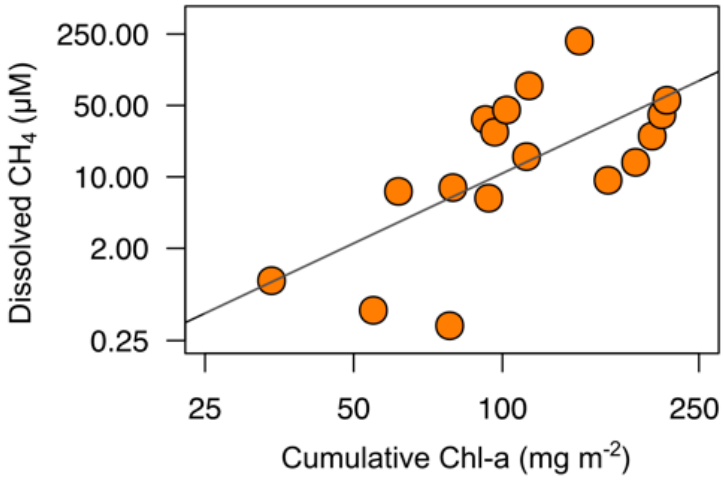

933

934 **Figure 5:** Power relationship between the depth-cumulative chlorophyll-a concentration and the concentration of dissolved CH_4 in the
935 anoxic waters during the stratification period (CH_4, µM = 3.0 10^{-4} Cumulative Chl-$a^{2.28}$, n= 17, adj R^2 = 0.40). Note that both axes are in
936 logarithmic scale. More statistical details in Table S2.

937

938

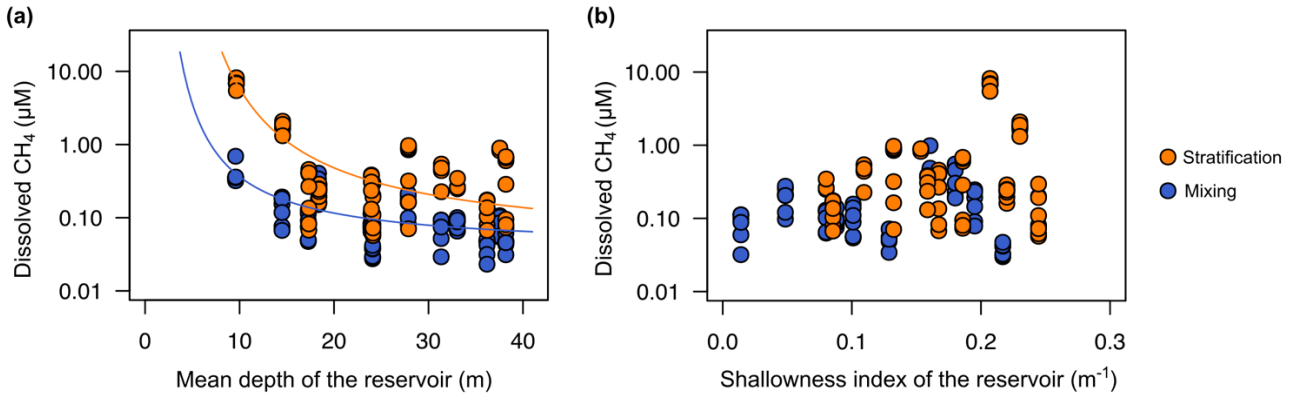

939

940 **Figure 6: Reservoir morphometry and the dissolved CH_4 concentration in the oxic zone.** (a) Exponential decay relationships of the
941 dissolved CH_4 concentration and the mean depth (m) during the stratification period (CH_4 = 4.0 10^{-2} e $^{(50.0/\text{ mean depth})}$, n= 78, adj R^2 = 0.95)
942 and the mixing period (CH_4 = 3.7 10^{-2} e $^{(22.9/\text{ mean depth})}$, n= 82, adj R^2 = 0.54). (b) Scatterplot of dissolved CH_4 concentration and the
943 reservoir shallowness index during the stratification period (p-value = 0.134) and the mixing period (n= 0.114). More statistical details in
944 Table S2.

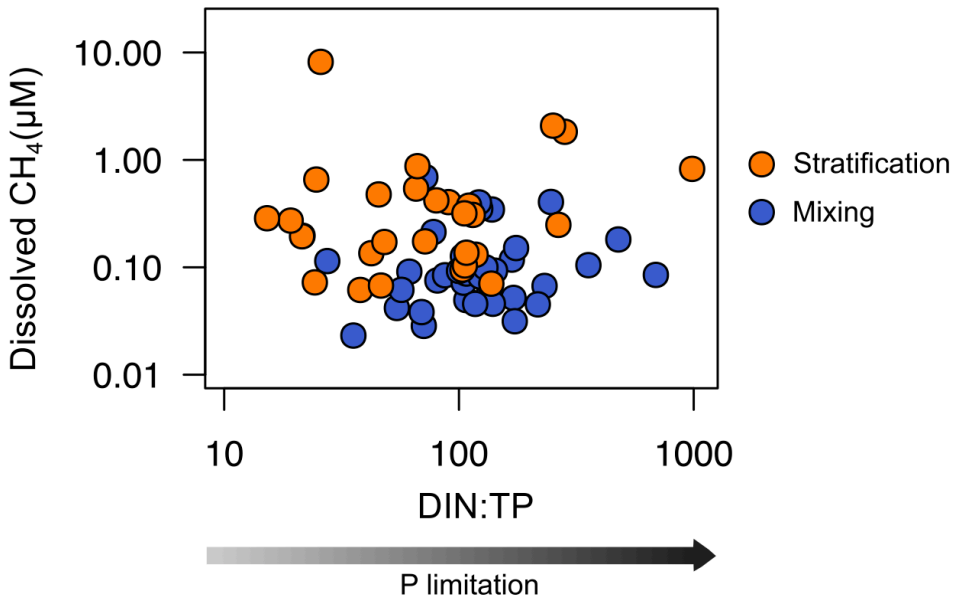

945

946 **Figure 7: Phosphorus limitation and the dissolved CH_4 concentration in the oxic waters.** Scatterplot of dissolved CH_4 concentration
947 and the ration between dissolved inorganic nitrogen (DIN) and the total phosphorus (TP) (µmol N : µmol P). Note the logarithmic scale in
948 both axes.

949

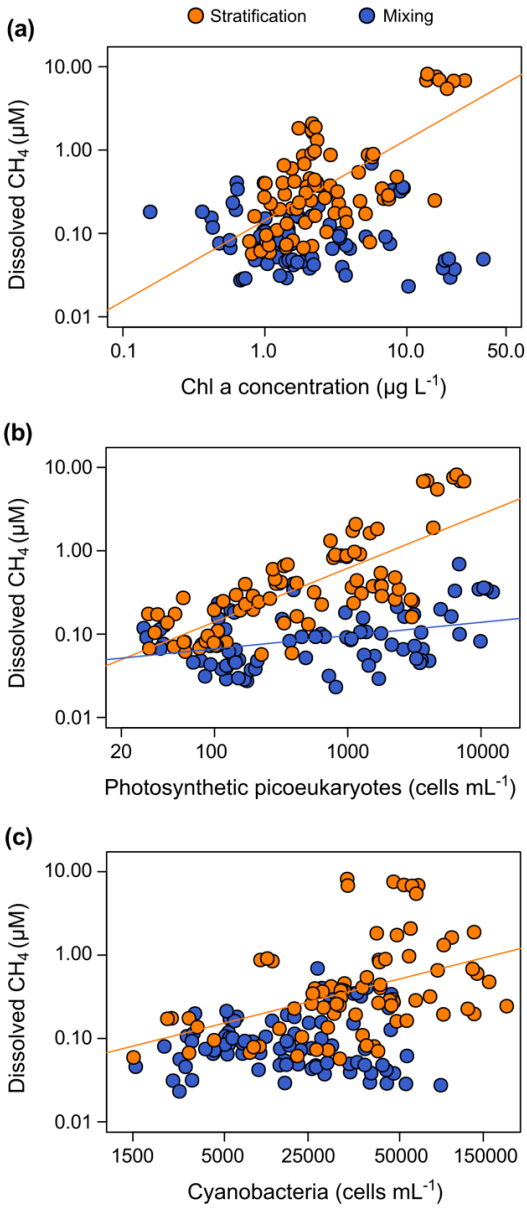

Figure 8: Phytoplanktonic variable coupled with the dissolved CH_4 concentration in the oxic waters. (a) The dissolved CH_4 concentration was significantly related to the chlorophyll-a concentration during the stratification period (p-value <0.001), but they were not related during the mixing period (p-value = 0.469). The relationship during the stratification period was a power function (CH_4, µM = 0.14 Chl-a$^{0.97}$; n = 78, adj R^2=0.40) **(b)** Relationships between dissolved CH_4 concentration and the abundance of photosynthetic picoeukaryotes (PPEs) during the stratification period (CH_4, µM = $7.2 \cdot 10^{-3}$ PPEs $^{0.65}$; n = 78, adj R^2=0.55, p-value <0.001) and the mixing period (CH_4, µM = $3.2 \cdot 10^{-2}$ PPEs $^{0.16}$; n = 82, adj R^2=0.12, p-value <0.001). **(c)** Relationship between dissolved CH_4 concentration and the cyanobacteria abundance (CYA, cell mL^{-1}). A power function described the relationship between the dissolved CH_4 and the CYA during the stratification period (CH_4, µM = $1.7 \cdot 10^{-3}$ CYA$^{0.53}$; n = 78, adj R^2=0.17, p-value <0.001). The relationship was not significant during the mixing period (p-value = 0.666).

960

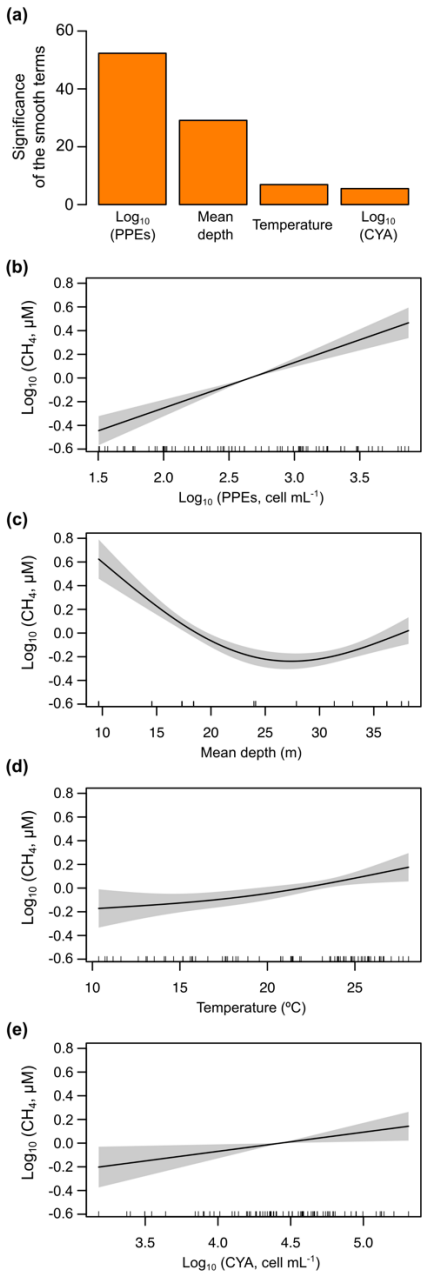

961

962 **Figure 9**. **Results of the Generalized Additive Model (GAM) fitted for the concentration of dissolved CH_4 in the oxic waters during**
963 **the stratification period. (a)** Bar plot showing the significance of the smooth terms from the fitted GAM model (F values). (**b-e**) Partial
964 response plots from the fitted GAM model showing the additive effects of the covariates on the dissolved CH_4 concentration: the
965 photosynthetic picoeukaryotes abundance (log_{10} PPEs) (**b**), the mean depth (**c**), the cyanobacteria abundance (log_{10} CYA) (**d**), and water
966 temperature (**e**). In partial response plots, the lines are the smoothing functions and the shaded areas represent 95% point-wise confidence
967 intervals. Rugs on x-axis indicate the distribution of the data. More details are provided in Table S3.

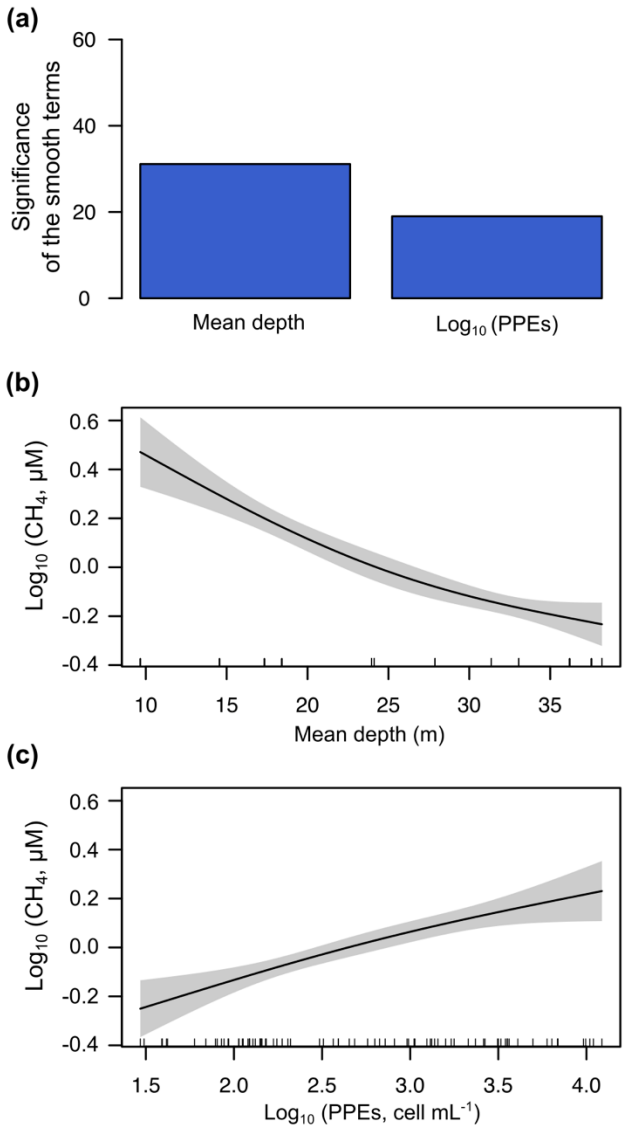

968

969 **Figure 10**. **Results of the Generalized Additive Model (GAM) fitted for the concentrations of CH_4 in the oxic waters during the**
970 **mixing period. (a)** Bar plot showing the significance of the smooth terms from the fitted GAM model (F values). (**b** and **c**) Partial
971 response plots from the fitted GAM model showing the additive effects of the covariates on the dissolved CH_4 concentration: the mean
972 depth (**b**) and the abundance of photosynthetic picoeukaryotes (log_{10} PPEs) (**c**). In partial response plots, the lines are the smoothing
973 functions and the shaded areas represent 95% point-wise confidence intervals. Rugs on x-axis indicate the distribution of the data. More
974 details are provided in Table S3.

975

976

977 **Table 1.** Geographical location and morphometric description of the study reservoirs.

Reservoir	Latitude (º, decimal degrees)	Longitude (º, decimal degrees)	Altitude (m)	Construction year	Reservoir area (km^2)	Reservoir capacity (hm^3)	Mean depth (m)	Shoreline development index (D_L)	Shallowness index (m^{-1})
Cubillas	37.27	-3.68	640	1956	1.94	18.74	9.66	2.00	0.21
Colomera	37.40	-3.72	810	1990	2.76	40.18	14.56	3.35	0.23
Negratín	37.56	-2.95	618	1984	23.51	567.12	24.12	5.90	0.24
La Bolera	37.76	-2.90	950	1967	2.89	53.19	18.40	4.05	0.22
Los Bermejales	36.99	-3.89	852	1958	5.95	103.12	17.33	2.90	0.17
Iznájar	37.26	-4.33	425	1969	26.13	981.12	37.55	5.76	0.15
Francisco Abellán	37.31	-3.27	942	1991	2.43	58.21	23.95	3.80	0.16
Béznar	36.92	-3.55	486	1986	1.60	52.90	33.06	2.65	0.08
San Clemente	37.86	-2.65	1050	1990	3.76	117.92	31.36	3.43	0.11
El Portillo	37.81	-2.79	920	1999	1.18	32.90	27.88	3.69	0.13
Jándula	38.23	-3.97	350	1932	8.43	321.99	38.20	7.10	0.19
Rules	36.86	-3.49	239	2003	3.06	110.78	36.20	3.09	0.09

978

979

Table 2. Sampling date, depth of the mixing layer (m), and mean values of the DOC, TN, and TP concentrations, DIN:TP ratio, and chlorophyll-a concentration in the water column of the study reservoirs during the stratification and the mixing period. The depth of the mixing layer was inferred from the temperature profile.

Reservoir	Period	Sampling Date	DOC (µM-C)	TN (µM-N)	TP (µM-P)	DIN:TP (µmol-N: µmol-P)	Chl-a (µg L^{-1})
Cubillas	Stratification	July 15, 2016	172.1	60.4	1.84	26	17.8
	Mixing	February 6, 2017	240.5	97.4	0.78	111	8.4
Colomera	Stratification	July 22, 2016	99.4	181.4	0.78	240	2.1
	Mixing	March 7, 2017	123.3	112.5	0.44	292	0.5
Negratín	Stratification	June 27, 2016	109.7	21.2	0.80	28	1.2
	Mixing	February 16, 2017	148.9	19.7	0.24	65	7.7
La Bolera	Stratification	June 28, 2016	123.7	17.3	0.61	25	2.0
	Mixing	April 8, 2017	107.4	34.4	0.15	178	0.8
Los Bermejales	Stratification	September 7, 2016	94.2	30.4	0.42	65	1.8
	Mixing	March 17, 2017	101.5	30.6	0.31	89	13.1
Iznájar	Stratification	September 9, 2016	116.8	278.5	0.39	729	5.1
	Mixing	March 15, 2017	147.5	260.0	1.16	393	1.1
Francisco Abellán	Stratification	September 28, 2016	90.6	27.8	0.28	200	1.9
	Mixing	March 21, 2017	118.0	28.5	0.47	63	1.1
Béznar	Stratification	October 7, 2016	74.3	74.2	0.68	227	6.0
	Mixing	February 23, 2017	121.6	105.6	0.95	104	3.7
San Clemente	Stratification	July 17, 2017	104.1	32.0	0.39	65	3.5
	Mixing	March 28, 2017	119.4	35.9	0.21	145	1.1
El Portillo	Stratification	July 18, 2017	78.0	22.8	0.17	102	2.4
	Mixing	March 30, 2017	76.4	34.4	0.26	109	1.7
Jándula	Stratification	July 24, 2017	359.9	34.3	0.78	43	2.3
	Mixing	April 5, 2017	399.4	46.2	0.37	104	1.2
Rules	Stratification	July 10, 2017	81.2	23.2	0.21	83	3.7
	Mixing	April 7, 2017	68.5	38.0	0.43	142	3.3

986

987 **Table 3.** Equations for the relationships between the phytoplanktonic variables and the dissolved CH_4 concentration in the
988 oxic waters. n.m. = not measured.

Driver	Period	n	Equation	Adj. R^2	p-value
Chl-a concentration ($\mu g\ L^{-1}$)	Stratification + Mixing	160	$CH_4\ (\mu M) = 0.12\ \text{Chl-a}^{0.44}$	0.11	< 0.001
	Stratification	78	$CH_4\ (\mu M) = 0.14\ \text{Chl-a}^{0.97}$	0.40	< 0.001
	Mixing	82	Not significantly related		0.469
Gross primary production (GPP, $g\ O_2\ m^{-3}\ d^{-1}$)	Stratification	12	Marginally significant		0.077
	Mixing	n.m.			
Net ecosystem production (NEP, $g\ O_2\ m^{-3}\ d^{-1}$)	Stratification	12	Not significantly related		0.536
	Mixing	n.m.			
Photosynthetic picoeukaryotes abundance (PPEs, cell mL^{-1})	Stratification + Mixing	160	$CH_4\ (\mu M) = 2.0 \cdot 10^{-2}\ \text{PPEs}^{0.35}$	0.19	< 0.001
	Stratification	78	$CH_4\ (\mu M) = 7.2 \cdot 10^{-3}\ \text{PPEs}^{0.65}$	0.57	< 0.001
	Mixing	82	$CH_4\ (\mu M) = 3.2 \cdot 10^{-2}\ \text{PPEs}^{0.16}$	0.12	< 0.001
Cyanobacteria abundance (CYA, cell mL^{-1})	Stratification + Mixing	160	$CH_4\ \mu M = 9.9 \cdot 10^{-4}\ \text{CYA}^{0.53}$	0.19	< 0.001
	Stratification	78	$CH_4\ \mu M = 1.7 \cdot 10^{-3}\ \text{CYA}^{0.53}$	0.17	< 0.001
	Mixing	82	Not significantly related		0.666

989

990